NPS ARCHIVE
1967
WADE, B.

PARAMETRIC AND EXPERIMENTAL ANALYSIS OF EJECTOR PERFORMANCE

BARTON SCOTT WADE

PARAMETRIC AND EXPERIMENTAL ANALYSIS

OF

EJECTOR PERFORMANCE

by

Barton Scott Wade
Lieutenant, United States Naval Reserve
B.S., Purdue University, 1961

Submitted in partial fulfillment of the
requirements for the degree of

MASTER OF SCIENCE

IN

AERONAUTICAL ENGINEERING

from the

NAVAL POSTGRADUATE SCHOOL
July 1967

S ARCHIVE
T
DE, B.

ABSTRACT

This investigation analyzes the operating characteristics of an ejector having a heated primary jet and a constant area mixing section. The effects of several key parameters are determined on the basis of idealized theory. Performance characteristics are described in terms of certain non-dimensional coefficients obtained by a systematic dimensional analysis.

In addition, experimental results obtained from a model ejector are presented. These results are in reasonable agreement with the theoretical analysis.

Suggestions are made for further improvements both in the theory and in the experimental facility.

ERRATA

page 10, line 17 should read "theoretical" vice "theoretcial"

page 12, para 2.2.a, line 3 should read "suitably" vice "suitable"

page 13, para 2.2.b, last line should read "suitably" vice "suitable"

page 22, line 7 should read "downstream" vice "down stream"

page 28, lines 1 and 2 should hyphenate the word "performance" between the m and the a

page 62, third line from bottom should read "of an" vice "on an"

page 68, eighth line from bottom should read "iteration" vice "interation"

page 87, item T_{T_2}/T_{T_1} is described as

"Average exit total temperatures.", this statement should read "Ratio of the secondary-to-primary total temperatures."

List of Symbols and throughout the thesis where C_p has been used as the symbol for specific heat at constant pressure, C_p should be changed to read c_p

TABLE OF CONTENTS

Section		Page
1.	INTRODUCTION	9
2.	THEORETICAL ANALYSIS	11
	2.1 Dimensional Analysis	11
	2.2 Definition of Dimensionless Coefficients	12
	2.3 Theoretical Development	16
3.	EXPERIMENTAL TEST FACILITY	19
	3.1 Primary Air System	19
	3.2 Secondary Air System	21
	3.3 Mixing Section	21
	3.4 Instrumentation	22
	3.5 Test Program	23
4.	DISCUSSION OF RESULTS	24
5.	RECOMMENDED MODIFICATIONS TO TEST FACILITY	27
6.	RECOMMENDATIONS FOR FURTHER STUDY	28
BIBLIOGRAPHY		57
APPENDIX A - Theoretical Analysis		58
APPENDIX B - Experimental Development		79

LIST OF ILLUSTRATIONS

Figure		Page
1.	H-S Diagram and Station Nomenclature	29
2.	Ejector Schematic	30
3.	Combustion Section	31
4.	Primary and Secondary Nozzle Arrangement	32
5.	Mixing Section Instrumentation Station	33
6.	Ejector Facility	34
7.	Ejector Facility	35
8.	Instrumentation	36
9.	Ideal Power Limits	37
10.	Ideal Pumping Limits	38
11.	Ideal Momentum Limits	39
12.	Comparison of Power Characteristics	40
13.	Comparison of Pumping Characteristics	41
14.	Comparison of Power Characteristics	42
15.	Comparison of Pumping Characteristics	43
16.	Comparison of Power Characteristics	44
17.	Comparison of Pumping Characteristics	45
18.	Comparison of Power Characteristics	46
19.	Comparison of Pumping Characteristics	47
20.	Comparison of Power Characteristics	48
21.	Comparison of Pumping Characteristics	49
22.	Comparison of Power Characteristics	50
23.	Comparison of Pumping Characteristics	51
24.	Comparison of Power Characteristics	52

Figure		Page
25.	Comparison of Pumping Characteristics	53
26.	Comparison of Power Characteristics	54
27.	Comparison of Pumping Characteristics	55
28.	Correlation between C_p and P_3/P_{T1}	56

LIST OF SYMBOLS

Symbol

P	Pressure
T	Temperature
ρ	Density
$\dot{m}$	Mass Flow Rate
H	Enthalpy
C_{pp}	Dimensionless Pumping Power Coefficient
C_{ps}	Dimensionless Suction Power Coefficient
C_{pt}	Dimensionless Total Power Coefficient
C_m	Dimensionless Momentum Coefficient
C_p	Dimensionless Driving Pressure Coefficient
C_s	Dimensionless Suction Pressure Coefficient
X	Mass Flow Rate Ratio ($\dot{m}_2/\dot{m}_1$)
A	AREA
C_p	Specific heat at constant pressure
M	Mach number
δ	Density ratio (ρ_2/ρ_1)
Φ	Dimensionless pressure rise across the mixing section (Eqn 16)
γ	Ratio of specific heats
μ	Compressibility factor defined by Eqn A-44

Subscript

T	Total or stagnation conditions
1	Primary fluid

Subscript

2	Secondary fluid
3	Mixing section exit
i	Inlet
m	Momentum

1. INTRODUCTION

An ejector, or jet pump, is a device which uses the relatively high energy of a small heated jet to produce a pressure rise in a relatively large mass flow. Such devices have many diversified applications. Jet pumps can be used as boundary layer control systems to delay the effects of flow separations. Air may be either blown over the lifting surface or sucked away from it. Similar devices, greatly enlarged, have also been employed as jet engine test cells where a large mass flow at high velocities is required. (Ref. 3). Further applications are in the fields of thrust augmentation and STOL/VTOL aircraft. (Ref. 6 and 7).

It was desired to study the effects of several key parameters upon which the performance of such ejectors depend. It became evident that before a specific parametric analysis could be performed, some meaningful set of performance coefficients should be developed which describe adequately the operation of an ejector. Such coefficients would also aid in the design of jet pumps in general. These performance coefficients have been derived on the basis of a logical dimensional analysis of the principal parameters which control the operation of such devices.

Once the coefficients were defined, a systematic study was performed to determine the effects which several key parameters have upon ejector operation.

This study is based upon the continuity, energy, and momentum equations as applied to the axi-symmetric, two-dimensional mixing of two concentric jets in a constant area duct. The final numerical results of this parametric analysis were determined by means of the Control Data Corporation 1604 digital computer. It should be noted that losses associated with friction and with incomplete mixing have been neglected, so that the results obtained represent the optimum performance levels which an ejector may approach but never exceed.

An experimental ejector, similar to that presented in Reference 2, was fabricated and installed in Building 216 at the Naval Postgraduate School, Monterey, California. A brief test program was conducted with this device in order to obtain an experimental comparison with the idealized theoretical trends.

Both the theoretcial analysis and the experimental test program are extensions of work initiated by Belter in Reference 1 and continued by Ridder and Summers in Reference 2. In the case of the parametric analysis, however, some results obtained in Reference 2 were found to be in error. Specifically, the tabulated mass flow ratios shown in Appendix C of this reference do not agree with values obtained by subsequent calculations. For this reason, along with the desire to develop a more simplified approach, the theoretical procedure presented in this report is basically original. The results obtained in Reference 2 apply only to compressible flows, while the methods presented herein may be applied to

either compressible or incompressible flows. The specific design of the experimental ejector suggested in Reference 2 was scaled down to approximately one-fourth the original linear size to meet cost and power supply limitations. Also, the actual ejector tested is of the variable inlet pressure type as compared to the variable back pressure system originally proposed.

Therefore, the goal of this study was to develop a more basic set of performance coefficients which adequately describe the operation of an ejector; to investigate the effect which several key parameters have upon these performance coefficients; and to obtain a comparison between experimental results and the idealized theory.

The author wishes to express his sincere appreciation for the invaluable assistance and guidance provided by Professor Theodore H. Gawain of the Naval Postgraduate School, Monterey, California.

2. THEORETICAL ANALYSIS

2.1 Dimensional Analysis

It may be seen from Figure 1 that the main parameters governing this problem are those which define the thermodynamic states of the primary fluid (P_{T1}, P_1, T_{T1}, T_1); the secondary fluid (P_{T2}, P_2, T_{T2}, T_2); and the fluid at the exit from the ejector (P_{T3}, P_3, T_{T3}, T_3). The amount of mass in each system and the geometric relation between the individual systems are also of great importance. For a thermodynamic system, in which electrical effects are

insignificant, four basic dimensions suffice to non-dimensionalize all possible physical characteristics of the system. For this study, the basic dimensional system of force, length, time, and temperature has been chosen. It is felt that by judicious selection of four reference parameters, which collectively represent the four basic dimensions, a more meaningful set of non-dimensional performance coefficients can be defined.

After analyzing the overall operation of an ejector, the following four parameters were chosen to represent the basic dimensional system:

		Symbol	Units
1.	The ambient density of the secondary fluid	ρ_{T2}	$\frac{FT^2}{L^4}$
2.	The ambient temperature of the secondary fluid	T_{T2}	Θ
3.	The mass flow rate of primary fluid	$\dot{m}_1$	$\frac{FT}{L}$
4.	The available enthalpy drop	H_a	$\frac{L^2}{T^2}$

Using these as a dimensional base, it is possible to express any other physical quantity in the form of a non-dimensionalized coefficient. (See Buckingham-Pi Theorem, Appendix A).

2.2 Definition of Dimensionless Coefficients

a. Pumping Power Coefficient

The pumping power coefficient is defined as the maximum available power at the exit from the constant area mixing section, suitable non-dimensionalized by means of the dimensional reference parameters mentioned above.

$$C_{pp} = \frac{(\dot{m}_1 + \dot{m}_2)H_3}{\dot{m}_1 H_a} \qquad (1)$$

b. Suction Power Coefficient

An ejector is capable of inducing a flow of secondary fluid from some pressure below that of static pressure at the exit from the mixing section. From a thermodynamic analysis (Appendix A) it can be shown that there is some ideal equivalent power required for this type of isothermal compression. The suction power coefficient is then defined as this equivalent power, suitable non-dimensionalized.

$$C_{ps} = \frac{\dot{m}_2 T_{T2} \Delta S_{i \to T2}}{\dot{m}_1 H_a} \qquad (2)$$

c. Total Power Coefficient

With an ejector developing power both in the form of available exit enthalpy and in the form of isothermal compression of the secondary fluid, it is appropriate to define the total power coefficient merely as the sum of these two outputs. The coefficient so established represents the maximum possible power developed by an ejector. Thus

$$C_{pt} = C_{pp} + C_{ps} \qquad (3)$$

d. Momentum Coefficient

The momentum coefficient is defined as the output momentum at the exit from the constant area mixing section, properly non-dimensionalized.

$$C_m = \frac{(\dot{m}_1 + \dot{m}_2)V_3}{\dot{m}_1 \sqrt{H_a}} \qquad (4)$$

It should be noted that the power coefficients C_{pp} and C_{ps}, being the ratios of output blowing and suction power, respectively, to available power, really represent the efficiencies of the system as a pump and as a suction device. The total power coefficient therefore represents the overall efficiency.

e. Driving Pressure Coefficient

The difference between the primary supply pressure (P_{T1}) and the static pressure at the exit plane (P_3) is non-dimensionalized by a suitable reference pressure. This then defines the driving pressure coefficient.

$$C_p = \frac{P_{T1} - P_3}{\rho_{T2} H_a} \tag{5}$$

f. Suction Pressure Coefficient

A second pressure parameter must also be defined for an ejector with a variable inlet (suction) pressure. As before, the difference between the secondary fluid total pressure (P_{T2}) and the exit static pressure (P_3) is properly non-dimensionalized to define the suction pressure coefficient.

$$C_s = \frac{P_{T2} - P_3}{\rho_{T2} H_a} \tag{6}$$

The major portion of this report deals with a compressible operating fluid and it became more convenient to use pressure ratios, $\frac{P_3}{P_{T1}}$ and $\frac{P_{T2}}{P_{T1}}$, as controlling parameters. There is, of course, a correlation between these ratios and the above pressure parameters as shown in Figure 28. Hence, the results of the study can be applied to either the compressible or incompressible situations.

g. Mass Flow Ratio

The rate of mass flow induced through the secondary system by the action of the primary jet is of primary importance in describing the pumping characteristics of an ejector. A non-dimensional mass flow is therefore defined as the secondary mass flow rate ($\dot{m}_2$) divided by the primary or supply mass flow rate.

$$X = \frac{\dot{m}_2}{\dot{m}_1} \tag{7}$$

h. Area Ratio

The geometrical factor which controls the performance of a jet pump is the physical size of the component systems. There is, therefore, a need to define certain size parameters to complete the non-dimensional description of an ejector system. As shown in Appendix A, the cross sectional area of the primary jet nozzle, and the constant area mixing section can be non-dimensionalized to give two area coefficients.

$$C_{A1} = A_1 \left(\frac{\rho_{T2}}{\dot{m}_1}\right) \sqrt{H_a} \tag{8}$$

and

$$C_{A3} = A_3 \left(\frac{\rho_{T2}}{\dot{m}_1}\right) \sqrt{H_a} \tag{9}$$

It is evident, however, that the individual size of each component is relatively unimportant and that the controlling geometric factor is simply the ratio of the mixing section area (A_3) to the primary nozzle area (A_1). For this reason, the above defined area coefficients were replaced by the ratio A_3/A_1 and C_{A3}.

With these coefficients, it is possible to describe the essential operating characteristics of an ejector system. This description is essentially independent of the operating fluid or of any absolute dimensional magnitudes. This method should aid in the specification of ejector design requirements.

2.3 Theoretical Development

This analysis is an investigation of the physical relationships which govern the operation of a jet pump. The resulting equations may be solved by a systematic iteration technique which can be performed on any digital computer.

Figure 1 shows the station locations and symbolic notation employed throughout this development.

The three basic conditions which must be satisfied for the constant area mixing of two streams of fluid in an axisymmetric duct are the equations of continuity, momentum, and energy. These equations, applied to the frictionless flow with uniform velocity distributions, are:

Continuity $$\dot{m}_1 + \dot{m}_2 = \dot{m}_3 \tag{10}$$

Momentum $$P_1A_1 + P_2A_2 - P_3A_3 = \dot{m}_3V_3 - \dot{m}_2V_2 - \dot{m}_1V_1 \tag{11}$$

Energy $$\dot{m}_1C_pT_{T1} + \dot{m}_2C_pT_{T2} = \dot{m}_3C_pT_{T3} \tag{12}$$

The detailed solution to these equations is given in Appendix A, and will not be covered here. The following is a summary of the resulting equations obtained, along with a listing of pertinent parameters. It is felt that in this manner the method of solution can more readily be shown.

Basic Equations

1. $$M_1 = \left[\left(\frac{2}{\gamma-1}\right)\left\{\left(\frac{P_{T1}}{P_{T2}}\right)^{\frac{\gamma-1}{\gamma}}\left(1+\frac{\gamma-1}{2}M_2^2\right)-1\right\}\right]^{1/2} \qquad (13)$$

2. $$\delta = \frac{\rho_2}{\rho_1} = \left(\frac{P_{T2}}{P_{T1}}\right)\left(\frac{T_{T1}}{T_{T2}}\right)\left[\frac{1+\frac{\gamma-1}{2}M_1^2}{1+\frac{\gamma-1}{2}M_2^2}\right]^{1/\gamma-1} \qquad (14)$$

3. $$X = \frac{\dot{m}_2}{\dot{m}_1} = \delta(K^2-1)\left(\frac{M_2}{M_1}\right)\left\{\left(\frac{T_{T2}}{T_{T1}}\right)\left[\frac{1+\frac{\gamma-1}{2}M_1^2}{1+\frac{\gamma-1}{2}M_2^2}\right]\right\}^{1/2} \qquad (15)$$

4. $$\Phi_i = \frac{P_3-P_2}{\rho_2 V_1^2}$$

or

$$\Phi_i = \left(\frac{1}{\delta\gamma M_1^2}\right)\left\{\left(\frac{P_3}{P_{T1}}\right)\left[1+\frac{\gamma-1}{2}M_1^2\right]-\left(\frac{P_{T2}}{P_{T1}}\right)\left[\frac{1+\frac{\gamma-1}{2}M_1^2}{1+\frac{\gamma-1}{2}M_2^2}\right]^{\gamma/\gamma-1}\right\} \qquad (16)$$

5. $$\Phi_M = \frac{1}{K^2}\left[\frac{1}{\delta}+\frac{\Delta P_1}{\rho_2 V_1^2}+\frac{X^2}{\delta^2(K^2-1)}-\frac{(1+X)(\mu\delta+X)}{\delta^2 K^2}\right] \qquad (17)$$

where

$$\frac{\Delta P_1}{\rho_2 V_1^2} = \frac{\left[1+\frac{\gamma-1}{2}M_1^2\right]^{\gamma/\gamma-1}}{\delta\gamma M_1^2}\left\{.528-\left(\frac{P_{T2}}{P_{T1}}\right)\frac{1}{\left[1+\frac{\gamma-1}{2}M_2^2\right]^{\gamma/\gamma-1}}\right\}$$

6. $$\frac{T_{T3}}{T_{T2}} = \left[\frac{\frac{T_{T1}}{T_{T2}}+X}{1+X}\right] \qquad (18)$$

7. $$\frac{\rho_3}{\rho_2} = \left[\frac{\frac{P_2}{\rho_2 V_1^2}+\Phi}{\frac{P_2}{\rho_2 V_1^2}}\right]\left(\frac{T_{T2}}{T_3}\right)\left[\frac{1}{1+\frac{\gamma-1}{2}M_2^2}\right] \qquad (19)$$

8. $$\mu = \frac{1}{\delta}\left[\frac{(1 + X)}{(\rho_{3/\rho_2})} - X\right] \qquad (20)$$

Known Parameters

1. $\frac{P_{T1}}{P_{T2}}$

2. $\frac{P_3}{P_{T1}}$

3. $\frac{T_{T1}}{T_{T2}}$

4. $K^2 = \frac{A_3}{A_1}$

Method of Solution

1. Assume a trial value for M_2.
2. Assume an initial trial value of μ equal to unity.
3. Calculate M_1, δ, X, Φ_i, and Φ_M.
4. Define an error function

   ERF = $\Phi_M - \Phi_i$.
5. Vary the trial value of M_2 until ERF = 0 for initial value of μ.
6. Using equations 6 thru 8 calculated a new value for μ.
7. With the new μ start M_2 iteration again.
8. Repeat until two successive values of M_2 are equal. This gives the proper value of M_2 and μ for the specified constant parameters.
9. Once M_2 and μ have been obtained, the performance coefficients may be calculated.

These computations are performed by the Fortran program JETPUMPI as shown in Appendix A.

3. EXPERIMENTAL TEST FACILITY

The model ejector employed for this study is essentially a scaled-down version of the design originally proposed by Ridder and Summers in Reference 2. A scale factor of approximately one-fourth was necessary to meet financial as well as power supply limitations; further, minor modifications were also made to the basic design.

The original proposal in Reference 2 called for a control valve to be installed at the exit from the mixing section. Such a valve would allow for controlling the static pressure at the exit to the ejector. Such a device is called a variable back pressure ejector. The actual test facility is open to atmospheric pressure at the exit plane and therefore not of the variable back pressure type. A control valve is installed in the secondary air system to facilitate controlling the secondary air total pressure. The pressure can be lowered from atmospheric to a partial vacuum. For this reason, the ejector tested is of the variable suction type.

The test model is comprised of three basic systems: The primary or high energy air system; the secondary or low energy system; and a variable length constant area mixing section.

3.1 Primary Air System

The primary air system, shown in Figure 2, is the energy source for the ejector. High pressure air is supplied

from a Pennsylvania Pump and Compressor Company HAE compressor and is delivered via a convergent nozzle to the mixing section. The total pressure, or pressure energy, supplied to the primary system can be controlled by a Cash-Acme pressure reducing and regulating valve assembly just upstream of the primary plenum chamber. In the present tests, the ejector was operated over a range of 4 to 25 psig although the compressor is capable of supplying air at pressures up to 100 psig.

The plenum chamber acts as a settling tank to minimize any turbulence or fluctuations in the primary flow. The air passes from the plenum through a bell-mouth into a two-inch pipe. Installed in the pipe is a stainless steel square edged orifice plate along with four flange static pressure taps and four vena contracta static pressure taps. An iron-constantan total temperature probe is also installed just upstream of the orifice plate. This arrangement makes it possible to measure flow rates in accordance with ASME standards. (Ref. 5).

Downstream of the orifice is a continuous burning combustion section. (Figure 3). This combustion section is fabricated of 304 stainless steel two-inch tubing. The actual combustion chamber is located in the middle of the section and a butterfly valve has been incorporated to control the amount of primary air passing through the combustion chamber. The remaining primary air by-passes the chamber, and in this manner the total temperature, or heat energy, of the primary air can be controlled.

After leaving the combustion section, the high energy air discharges into the stainless steel mixing section through a convergent nozzle. The nozzle, as depicted in Figure 4, is located inside the secondary air system plenum chamber in such a way as to develop two concentric jets at the entrance to the mixing section.

3.2 Secondary Air System

The high energy jet issuing from the primary nozzle induces a flow of secondary air, from ambient conditions, through a bell mouth inlet into a three-inch standard pipe. A square edged orifice system is installed in the pipe for mass flow rate determination. The system is identical to that employed for the primary air.

Downstream of the mass flow rate measuring station, there is a three-inch gate valve. By varying the setting of this valve, the total pressure of the secondary air can be decreased below atmospheric. In this manner the operation of a suction type ejector can be simulated.

The secondary air then enters a plenum chamber, the purpose of which is to provide more nearly uniform and axisymmetric inlet conditions. The air then enters the mixing section through a convergent nozzle.

3.3 Mixing Section

Both the primary and secondary jets meet at the entrance to a constant area duct or mixing section. Mixing sections of three different diameters are available. Also, primary nozzles of three different sizes can be installed. Therefore,

nine different area ratios can be obtained. For this study, however, only one mixing section was used.

The section employed is made of nominal two-inch stainless steel tubing (ID = 2.25 inches), fabricated in three sections. By varying the combination of sections, a range of L/D ratios from two to ten can be obtained. L is the length of tubing down stream of the nozzle exit.

Five instrumented stations (Figure 5) are equally spaced along the length of mixing section. At each station are two averaging static pressure wall taps (1/32" diameter). There is also a 1/8-inch hole with a boss assembly for obtaining pitot static and total temperature surveys at each station.

For normal applications, a diffuser would be installed downstream of the mixing section to convert any velocity at the exit to a static pressure rise. For this study, however, a diffuser was not incorporated since the mixing process was of prime interest.

3.4 Instrumentation

All pressures were obtained from a 94-inch mercury manometer bank with the exception of the ΔP across each orifice plate and the exit traverse pressures. The ΔP's were read from a water micromanometer calibrated in centimeters, while the traverse pressure was read in inches of water from a 48-inch single tube manometer. The two temperatures upstream of the orifice plates and the exit total temperature were measured with iron-constantan thermocouples with a Leeds and Northrup millivolt readout.

The mass flow rates were calculated based upon Reference 4, as shown in Appendix B. The total temperatures recorded upstream of the orifice plates were assumed to be the static temperature for these calculations. Although the mass flow measuring system is equipped with both flange and vena contracta static pressure taps, the pressures measured with the flange taps were used in the determination of the mass flow rates.

The overall test ejector and instrumentation system are shown on Figures 6, 7, and 8.

3.5 Test Program

Once the model ejector was fabricated and installed in Bldg. 216 at the Naval Postgraduate School, the system underwent several trial runs in order to eliminate all air leaks and to check out the instrumentation system. Upon completion of these trial runs, nine runs were made to collect the necessary raw data.

The first four runs were made with an area ratio of 10.125:1, while the last five were with an area ratio of 20.25:1. All runs were with a temperature ratio of unity since the combustion section was not in operation due to the lack of fuel and a calibrated fuel flow orifice.

A typical run consisted of the following steps:

1. Establish a given P_3/P_{T1} ratio.
2. Set the secondary control valve in the full open position.
3. Record all data, including an eight station traverse for both pitot-static and total temperature profiles.

4. Close the secondary control valve in four steps and record the new data at each step.

For an area ratio of 10.125:1, four different values of P_3/P_{T1} were used. These were values of 0.4, 0.5, 0.6, and 0.8. For the 20.25:1 ratio values of 0.3, 0.4, 0.5, and 0.6 were used. In addition, two additional runs were made so that a check could be made upon the repeatability of the system. These runs were at an A_3/A_1 of 10.125 and P_3/P_{T1} of 0.4 and 0.5. The results of these reruns are shown in Figures 16, 17, 18, and 19.

The raw data was then reduced as outlined in Appendix B. The final numerical results were obtained by means of the IBM 360 digital computer through the Fortran program EJECTOR.

4. DISCUSSION OF RESULTS

Figures 9 thru 11 show the ideal performance limits for an ejector with zero suction, all output being in the form of blowing. It was found that a slight decrease in secondary total pressure below ambient resulted in a large decrease in mass flow ratio. Also, at zero suction, the total power coefficient, and hence, the overall efficiency were maximum. For this reason, these curves depict the maximum possible performance levels for this study. As previously mentioned, these figures represent the optimum performance levels which an ejector may approach but never exceed.

Figure 9 is an overall mapping of the pumping power performance. It should be pointed out that although the value of C_{pp} decreases with increases in temperature ratio (T_{T1}/T_{T2}), the value of the absolute power will increase. The apparent indicated decrease is actually a loss in efficiency.

Similarly, Figure 10 summarizes the relationship between mass flow ratio and the pressure coefficient. It is seen that C_p tends to decrease more or less sharply as the mass flow ratio is increased. This is in contrast to the power trends where the effect of increasing mass flow ratio is not quite so severe. It is also of interest to note that for a given temperature ratio, the range of C_p is practically independent of area ratio.

The limiting values for output momentum coefficient are plotted in Figure 11, with mass flow ratio as the independent variable. This figure shows that an increase in temperature ratio has little effect upon the output momentum, C_m. An increase in area ratio will, however, result in an increase in C_m.

The detailed comparison between the theoretical trends and the experimental results is given in Figures 12 thru 27. The graphs depict the performance of an ejector, both as a power producing device (C_{pp} and C_{ps}), and as a pump (C_p and C_s). Each set of curves is for a given value of P_3/P_{T1} and A_3/A_1. The parameter C_{A3} is considered to be of secondary importance, and detailed values are therefore not presented;

however, the range of C_{A3} values was from 225 to 475. All curves are for a temperature ratio of unity since the combustion chamber was not in operation for these tests.

It is readily apparent that the experimental results follow the theoretical trends although, as expected, there is considerable deviation in actual magnitudes. The power curves (C_{pp} and C_{ps}) show that the greatest deviation from the ideal case is a result of a decrease in attainable flow rates. This can be attributed to friction and mixing losses in the experimental system and also to inlet losses. These effects are shown as ΔX friction and ΔX inlet, respectively. The inlet losses result from a decrease in secondary total pressure. This drop in total pressure makes it impossible to obtain true zero suction operation, and hence, decreases the performance level.

The pumping characteristic curves also show the effect of friction, mixing, and inlet losses. The approximately constant deviation between the actual and theoretical values of suction pressure coefficient is the result of friction and mixing effects. It reduces the maximum flow capability by the amount ΔX friction as indicated on the diagrams. The remaining loss in mass flow ratio is associated with flow resistance thru the inlet valve of the secondary system, and is denoted by ΔX inlet. Since the controllable parameter for each test was the pressure ratio P_3/P_{T1}, the agreement between the theoretical and experimental values of C_p is necessarily close.

In general it can be said that the analytical approach employed for this study yields a reasonable overall picture of ejector performance trends. The experimental results are in agreement with the parametric analysis in regard to the qualitative effect of several key parameters upon ejector performance. The agreement between theory and experimental results is encouraging; however, a somewhat more detailed analysis which includes friction and mixing effects will clearly be necessary before actual performance levels can accurately be predicted.

5. RECOMMENDED MODIFICATIONS TO TEST FACILITY

The experimental model has proven to be useful and reliable for studying ejector performance. It is felt that the losses shown for this model can be reduced with the following modifications:

a. Install a more efficient valve in the secondary air system to reduce the pressure loss through the valve.

b. Increase the size of the secondary plenum chamber, or add some form of baffle system to provide a more uniform velocity distribution at the entrance to the mixing section. This requirement became apparent at high values of C_s, where the flow at the exit plane was not axi-symmetric.

For an actual ejector, the inlet losses will be reduced since the length of plumbing associated with the flow rate measuring system will not be required.

6. RECOMMENDATIONS FOR FURTHER STUDY

In order to develop a method whereby the actual performance levels of an ejector system can be adequately predicted, the following extensions to present work are strongly recommended:

a. Extend the present theory to include the effects of friction and mixing losses. This can be accomplished by the addition of a friction term to the momentum equation and by developing a suitable shape factor to better describe the mixing process.

b. Complete the incorporation of a fuel system in the existing ejector. By installing a fuel flow regulating valve and flow meter, the existing facility will be capable of producing a wide range of temperature ratios.

c. Conduct a more detailed experimental test program in which velocity traverses are taken at the five stations along the mixing section. Such a study will provide a better understanding of the mixing process and should aid in the determination of the shape factor previously mentioned.

d. Investigate the actual application of ejector systems to boundary layer control work. Such an investigation could be made utilizing the existing ejector in conjunction with a series of aerofoils. By installing the aerofoils in a wind tunnel the effect of the ejector suction or blowing upon flow separation could be studied.

Figure 1

H-S DIAGRAM AND STATION NOMENCLATURE

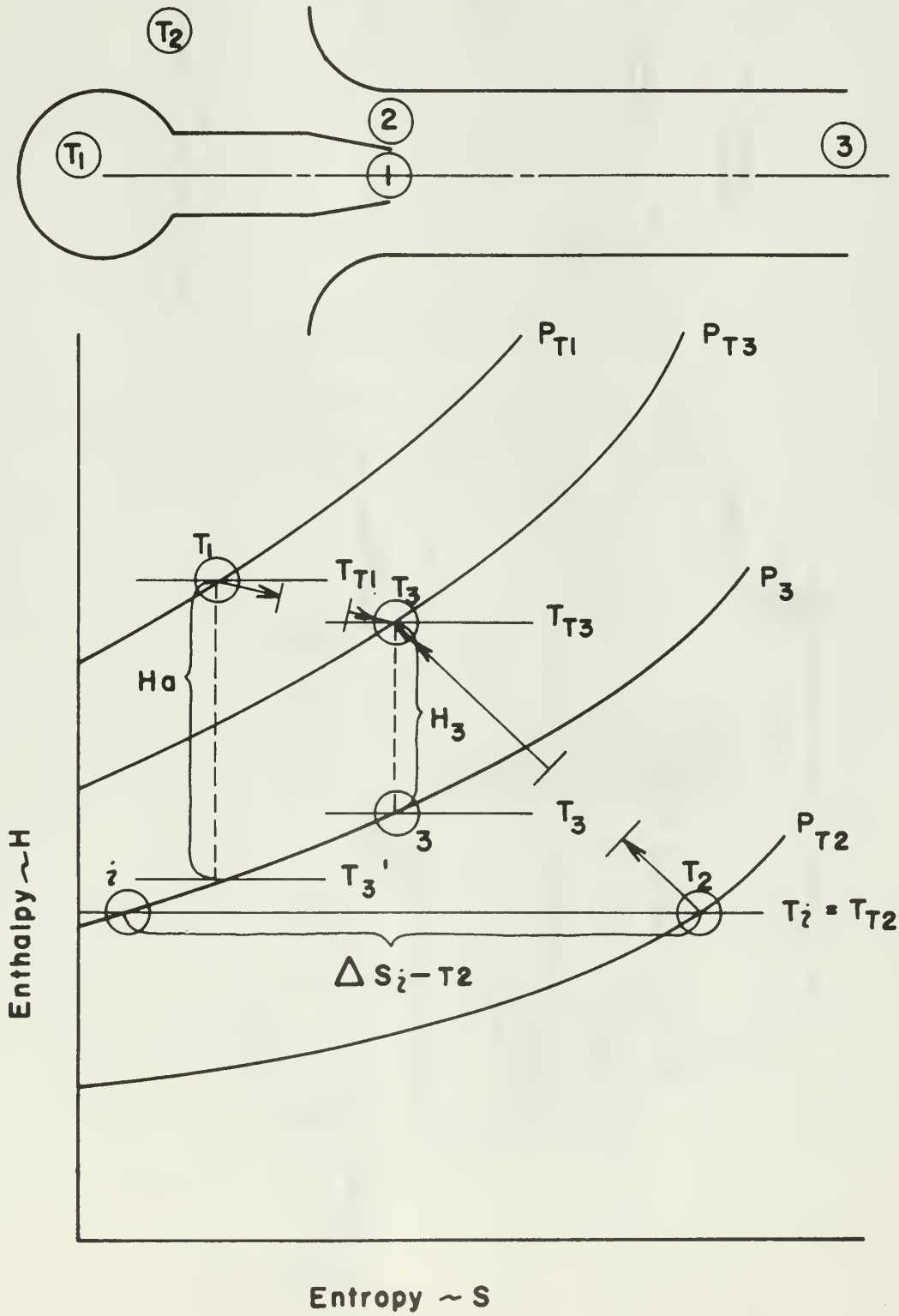

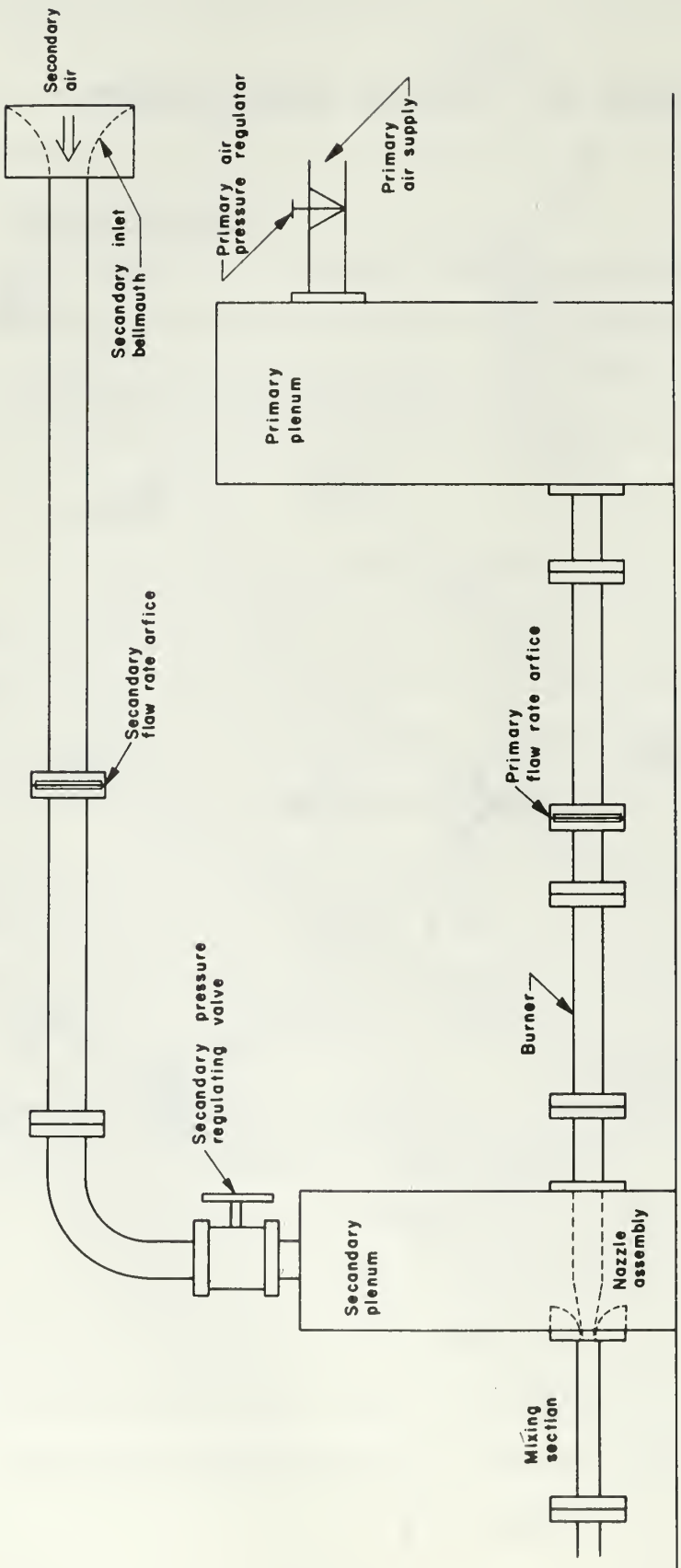

FIG. 2 EJECTOR SCHEMATIC

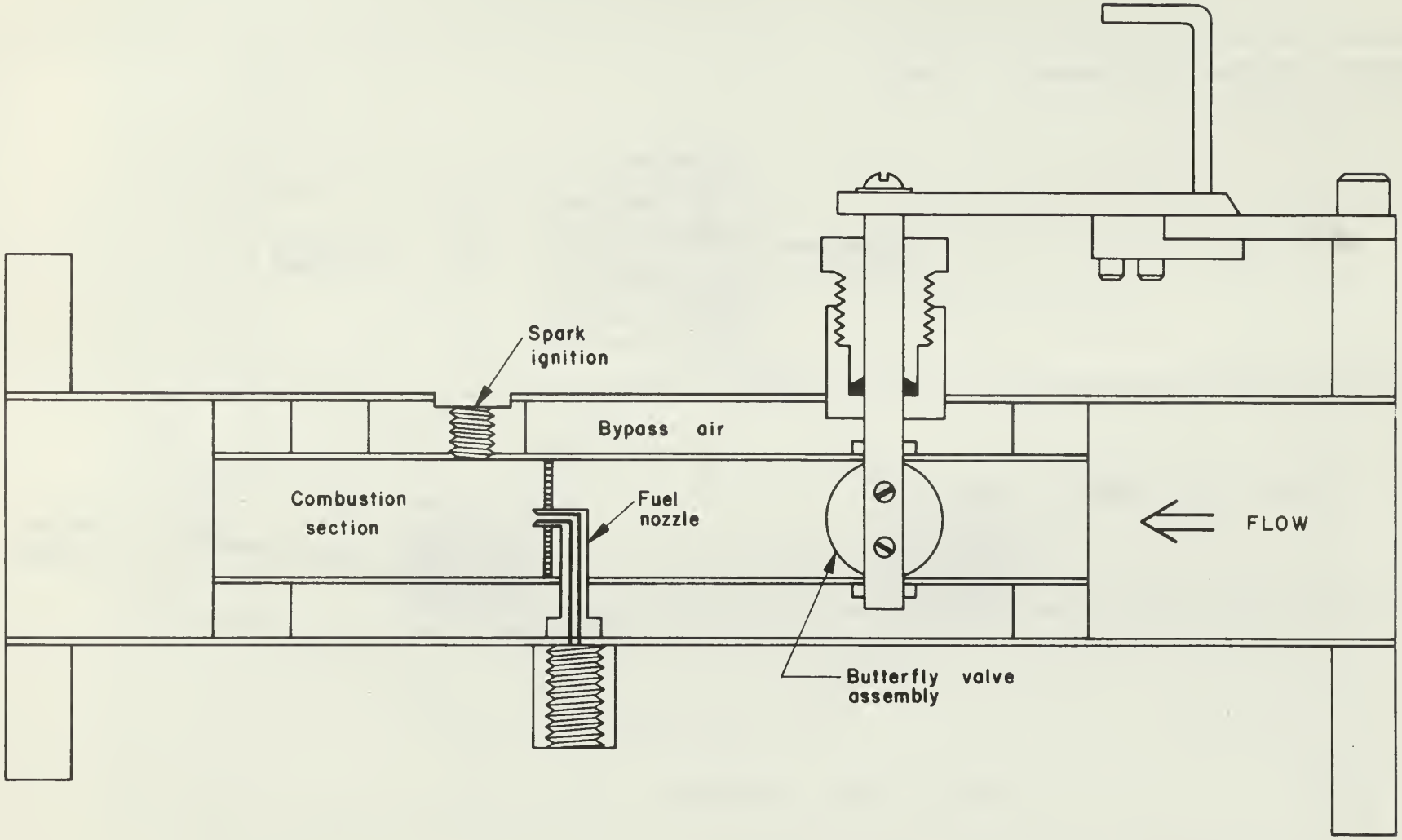

FIG. 3 COMBUSTION CHAMBER

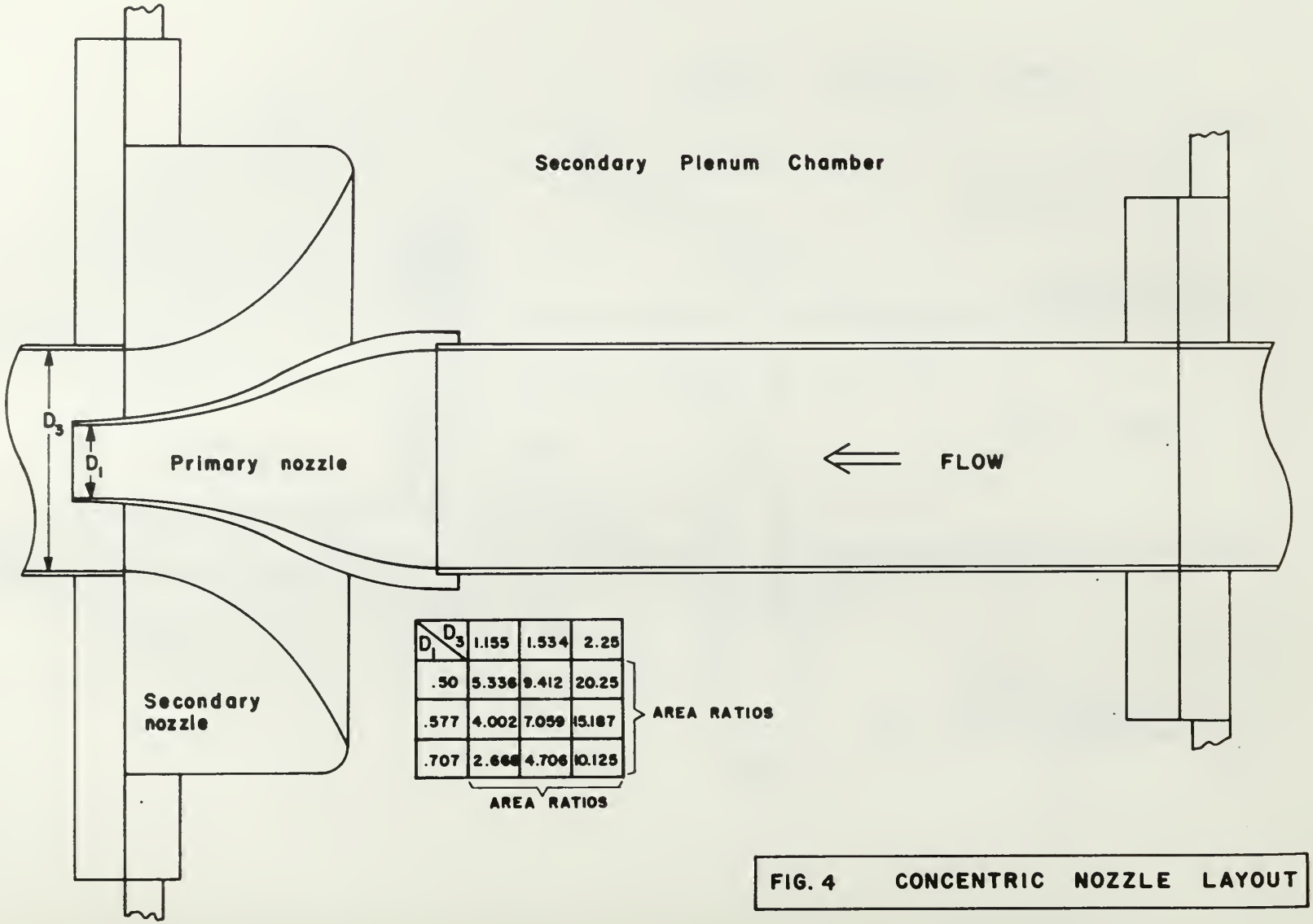

D_1 \ D_3	1.155	1.534	2.25
.50	5.336	9.412	20.25
.577	4.002	7.059	15.187
.707	2.666	4.706	10.125

AREA RATIOS

AREA RATIOS

FIG. 4 CONCENTRIC NOZZLE LAYOUT

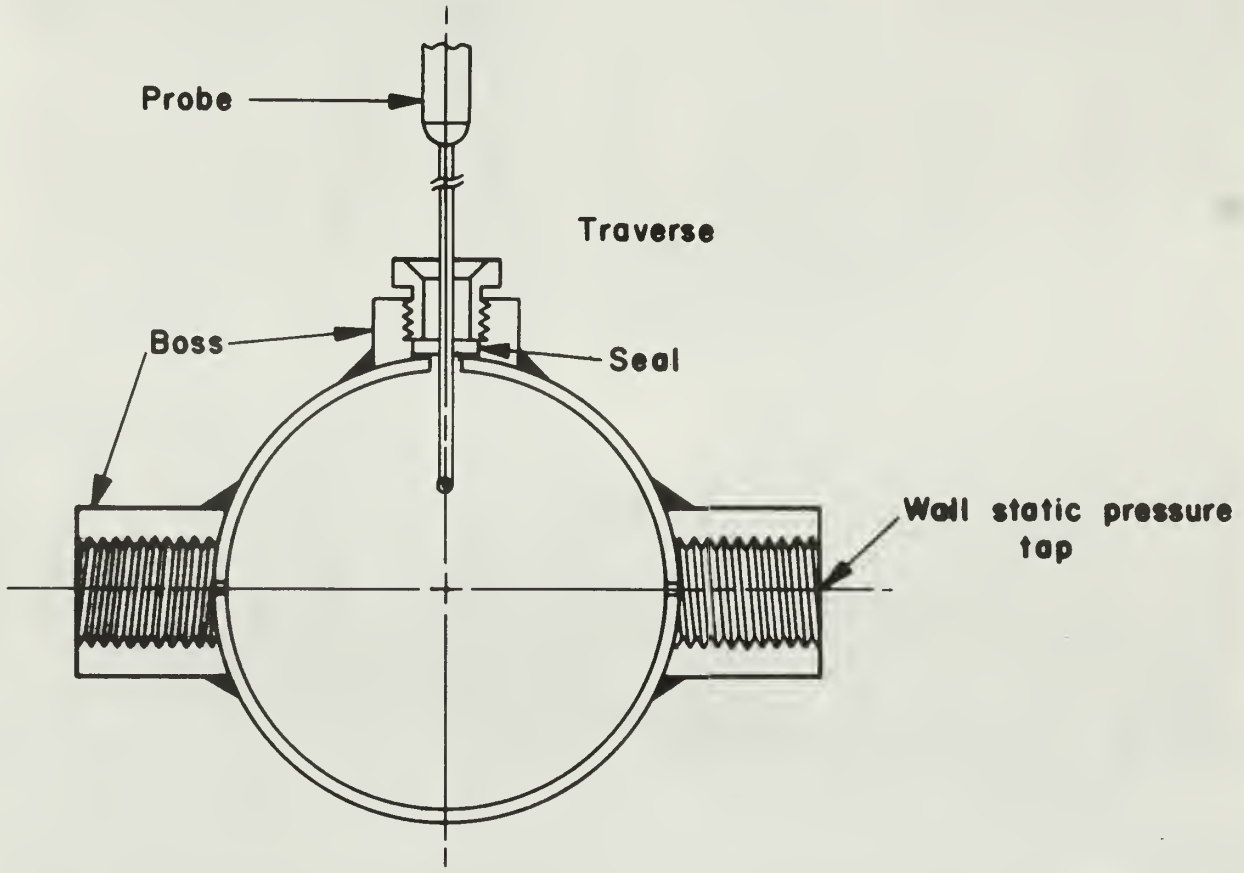

FIG. 5 MIXING SECTION INSTRUMENTATION STATION

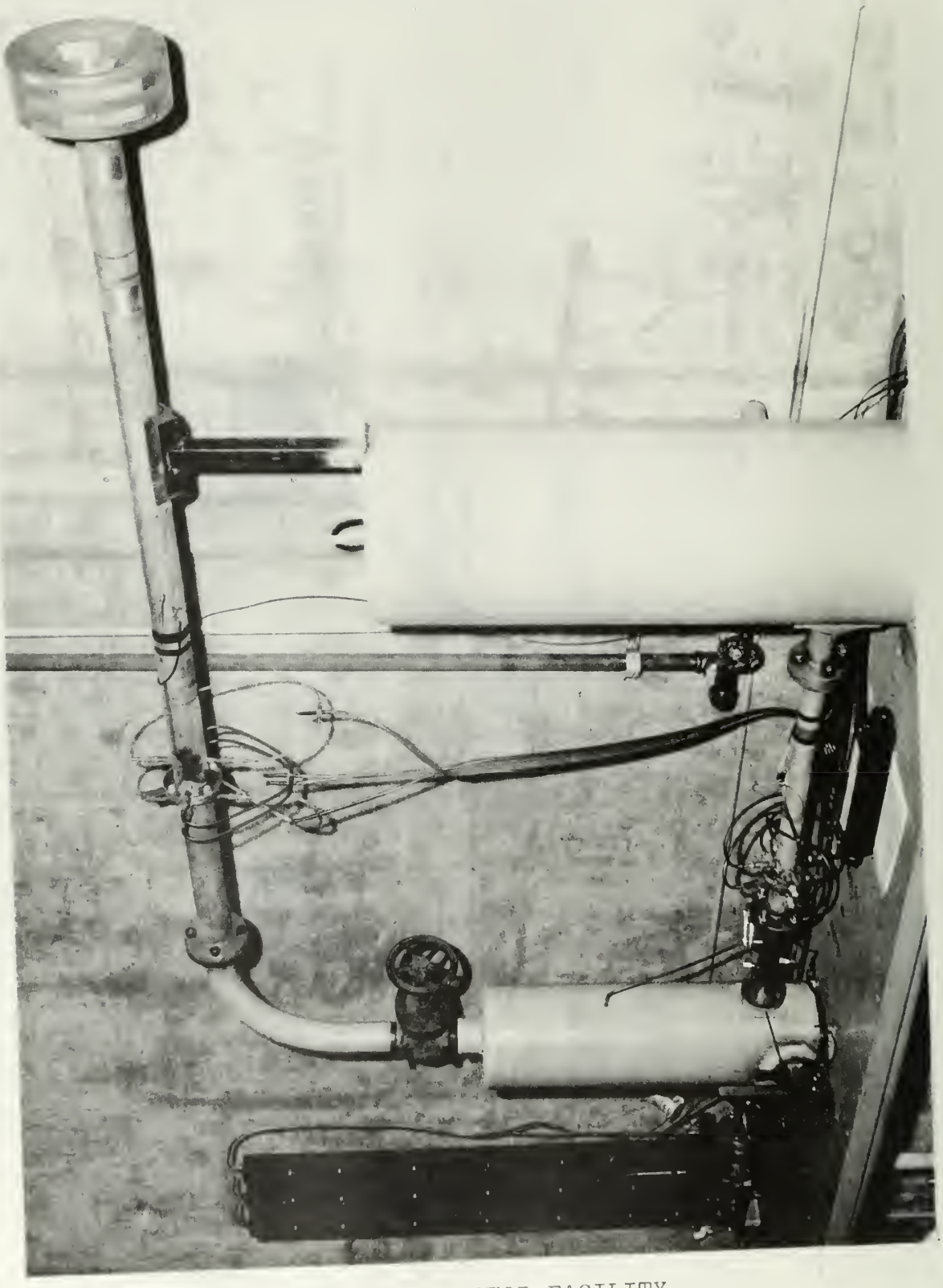

FIGURE 6 EJECTOR FACILITY

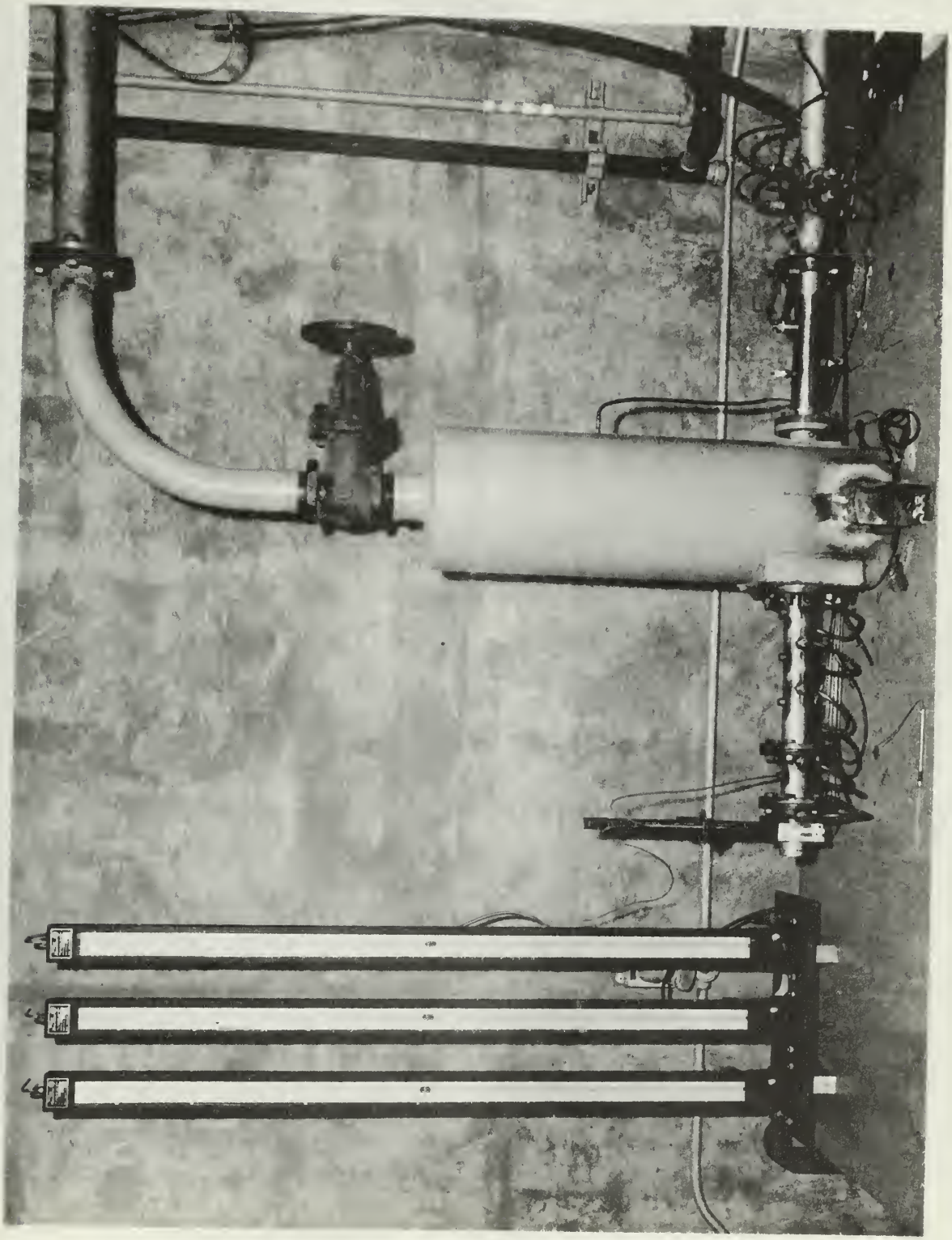

FIGURE 7 EJECTOR FACILITY

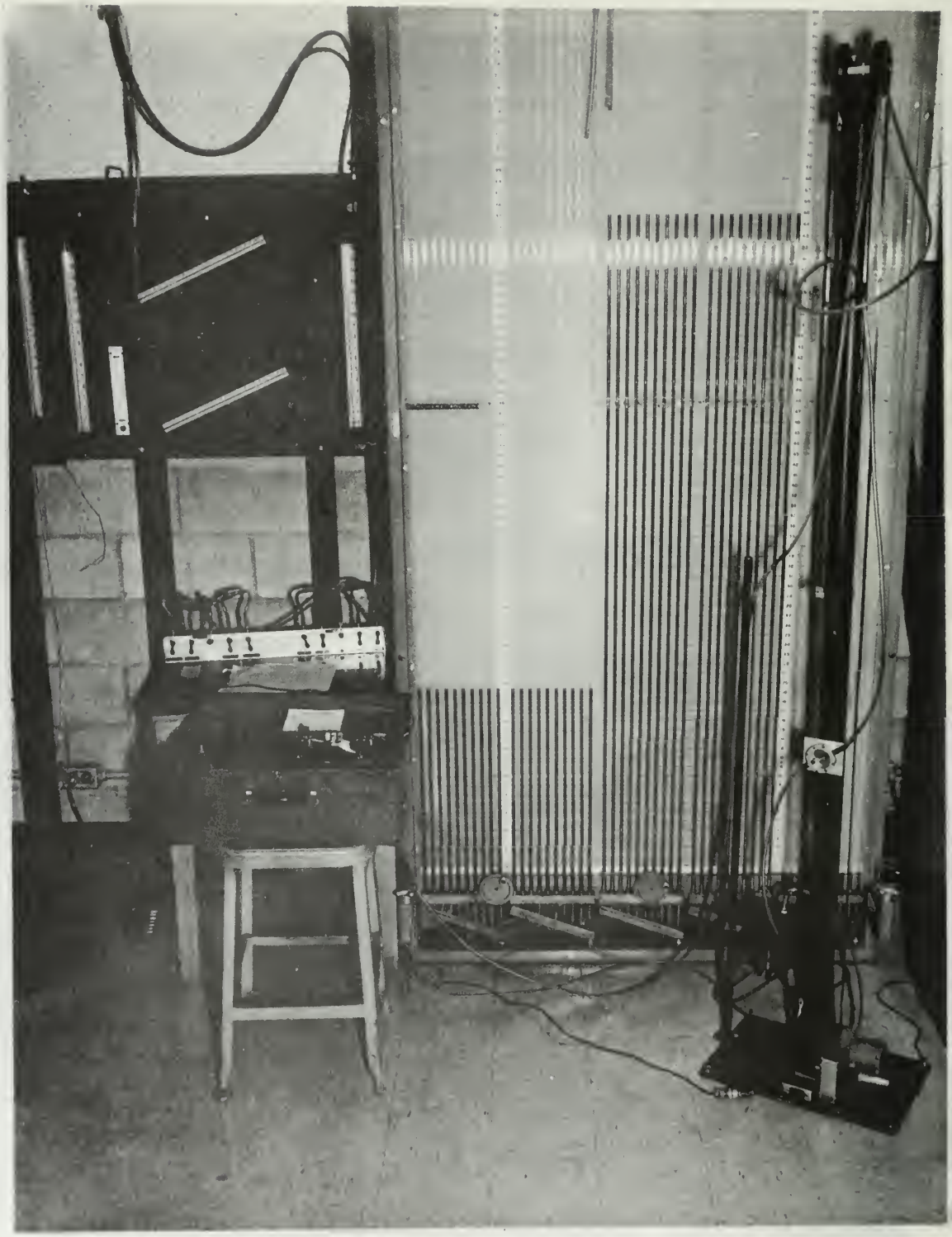

FIGURE 8 INSTRUMENTATION

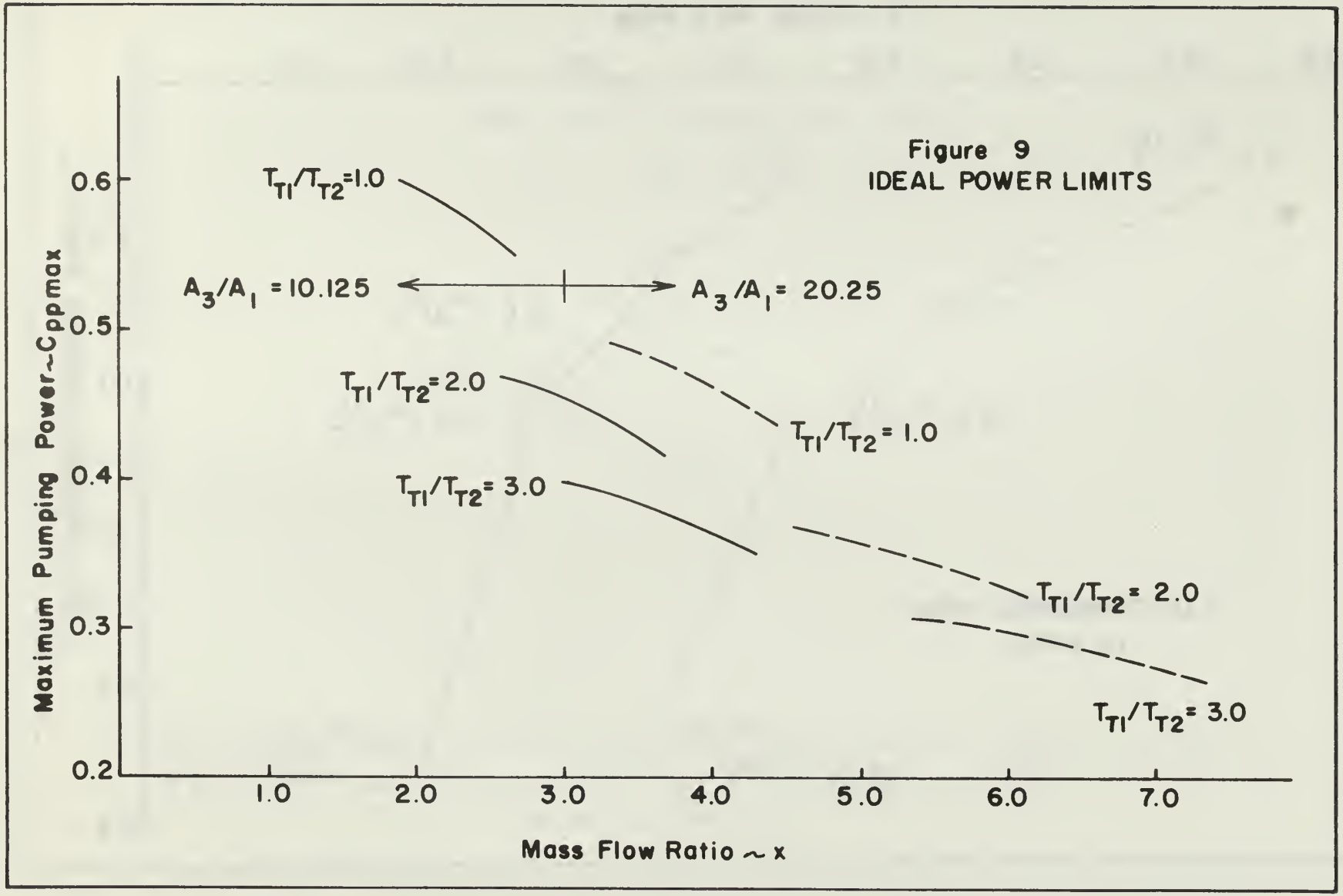
Figure 9
IDEAL POWER LIMITS
Maximum Pumping Power ~ Cppmax
0.6
0.5
0.4
0.3
0.2
T_{T1}/T_{T2}=1.0
A_3/A_1 = 10.125
A_3/A_1 = 20.25
T_{T1}/T_{T2}= 2.0
T_{T1}/T_{T2}= 1.0
T_{T1}/T_{T2}= 3.0
T_{T1}/T_{T2}= 2.0
T_{T1}/T_{T2}= 3.0
1.0
2.0
3.0
4.0
5.0
6.0
7.0
Mass Flow Ratio ~ x

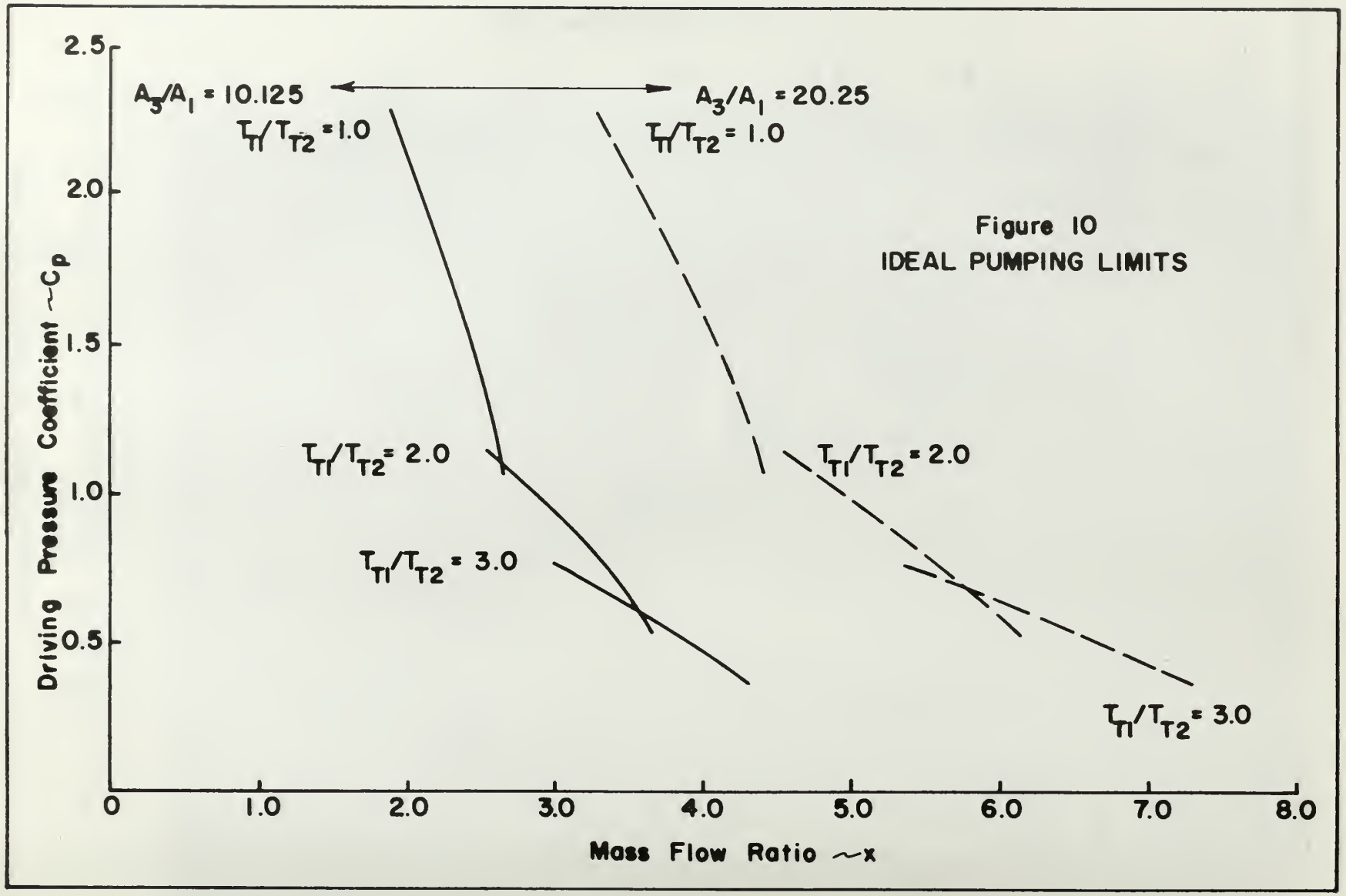

Figure 10
IDEAL PUMPING LIMITS

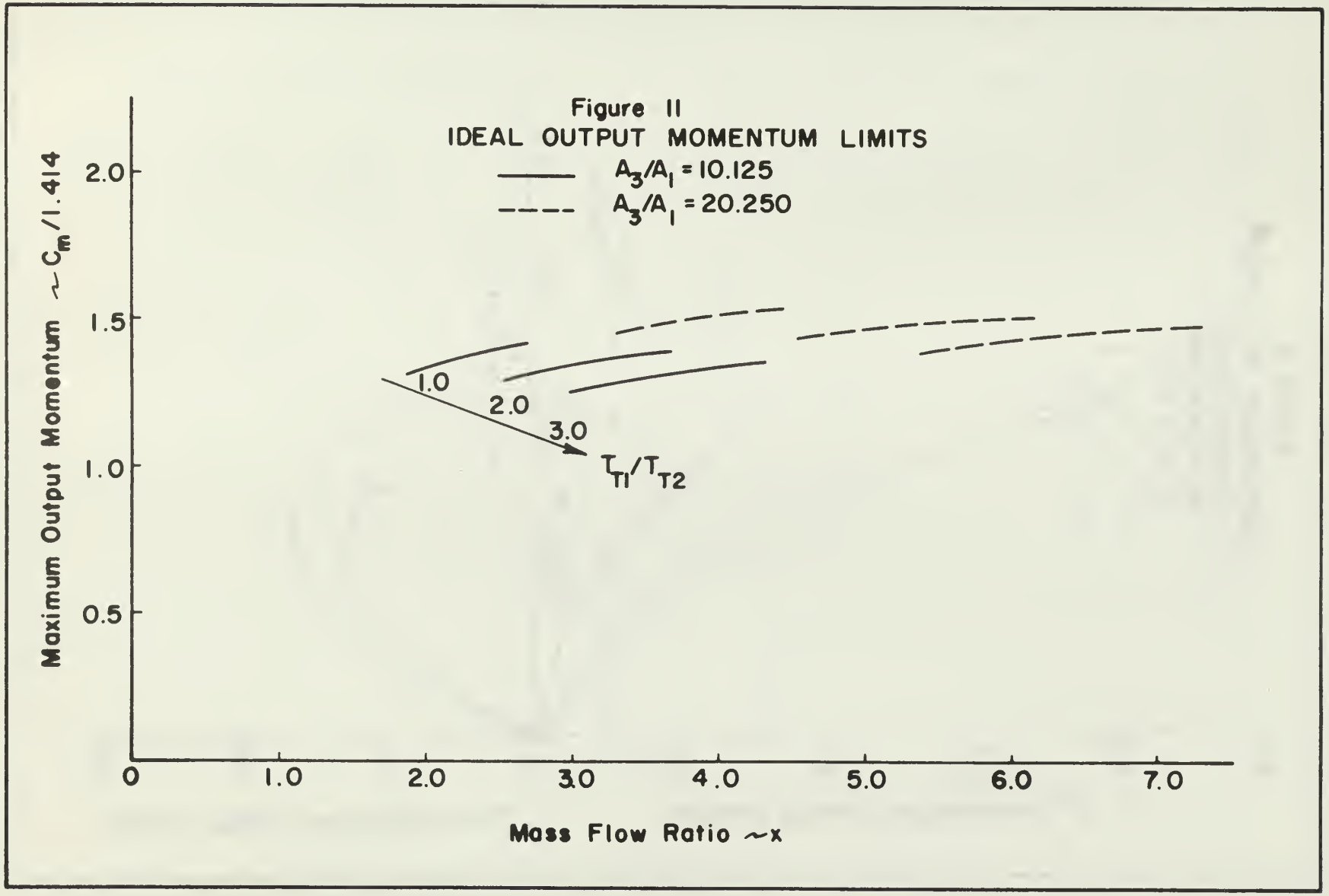
Figure 11
IDEAL OUTPUT MOMENTUM LIMITS
$A_3/A_1 = 10.125$
$A_3/A_1 = 20.250$
Maximum Output Momentum $\sim C_m/1.414$
2.0
1.5
1.0
0.5
1.0
2.0
3.0
T_{T1}/T_{T2}
0
1.0
2.0
3.0
4.0
5.0
6.0
7.0
Mass Flow Ratio $\sim x$

Figure 12

COMPARISON OF POWER CHARACTERTICS

$A_3/A_1 = 10.125$

$P_3/P_{T1} = 0.80$

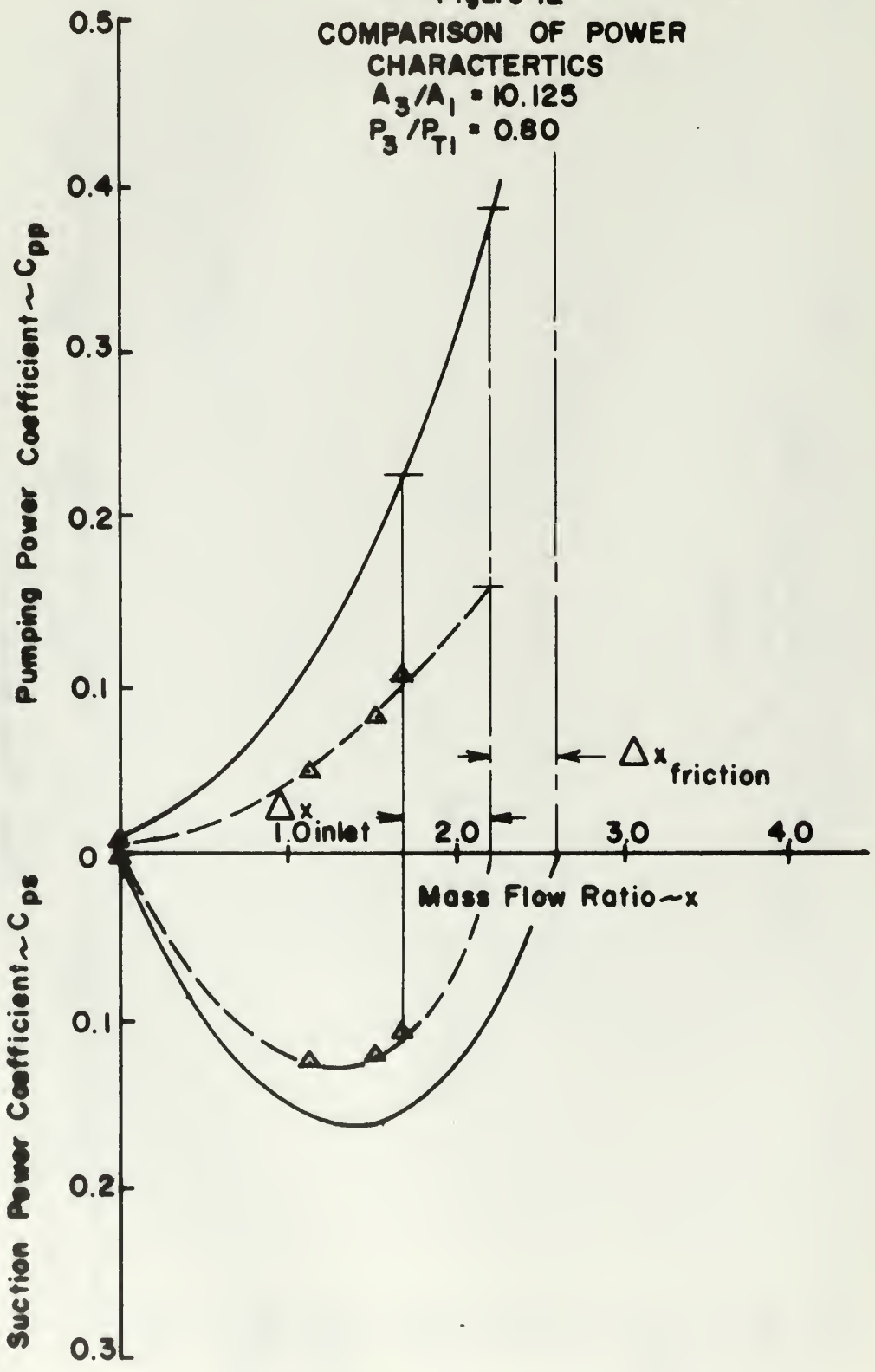

Figure 13

COMPARISON OF PUMPING CHARACTERISTICS

$A_3/A_1 = 10.125$

$P_3/P_{T1} = 0.80$

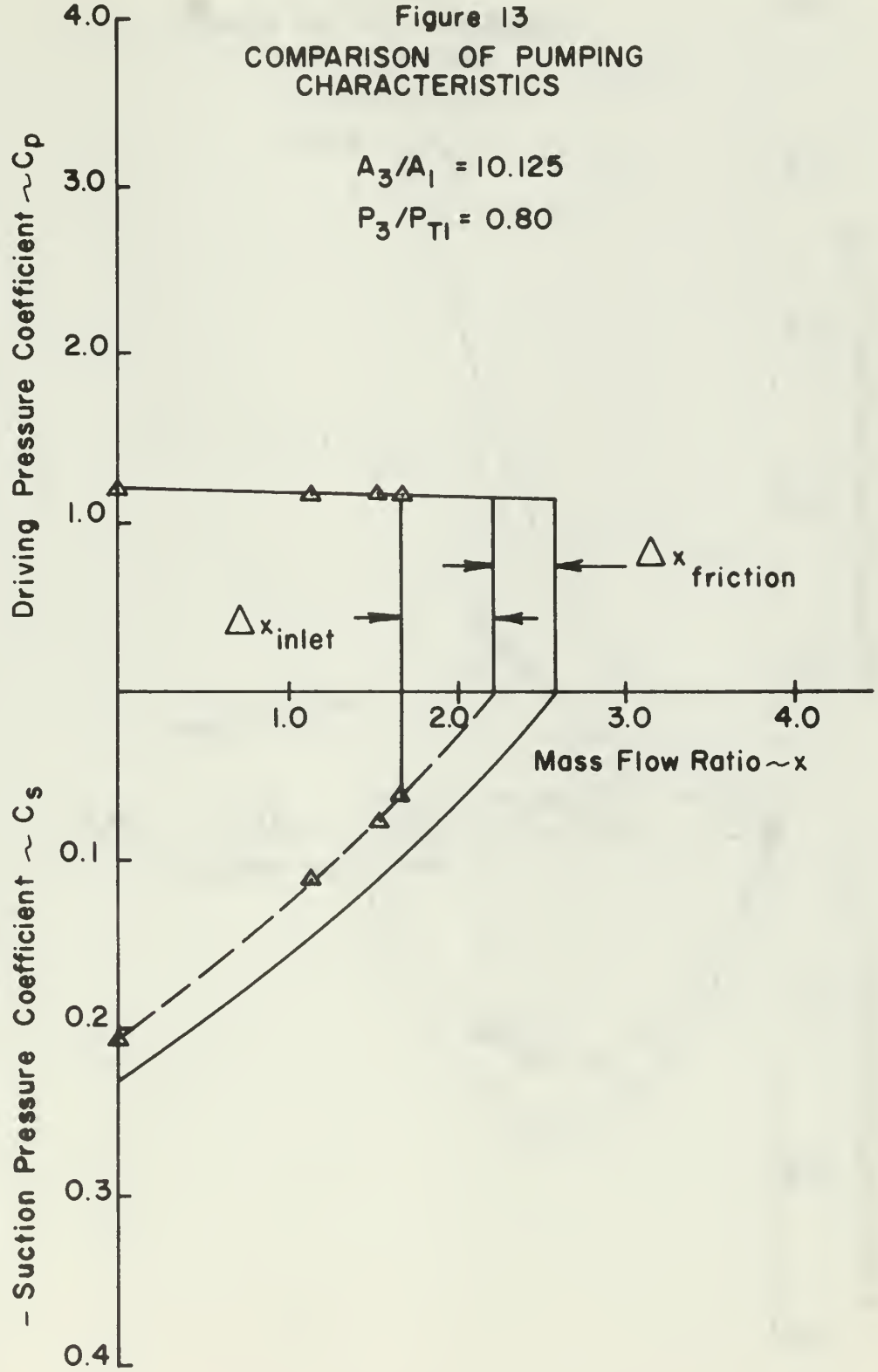

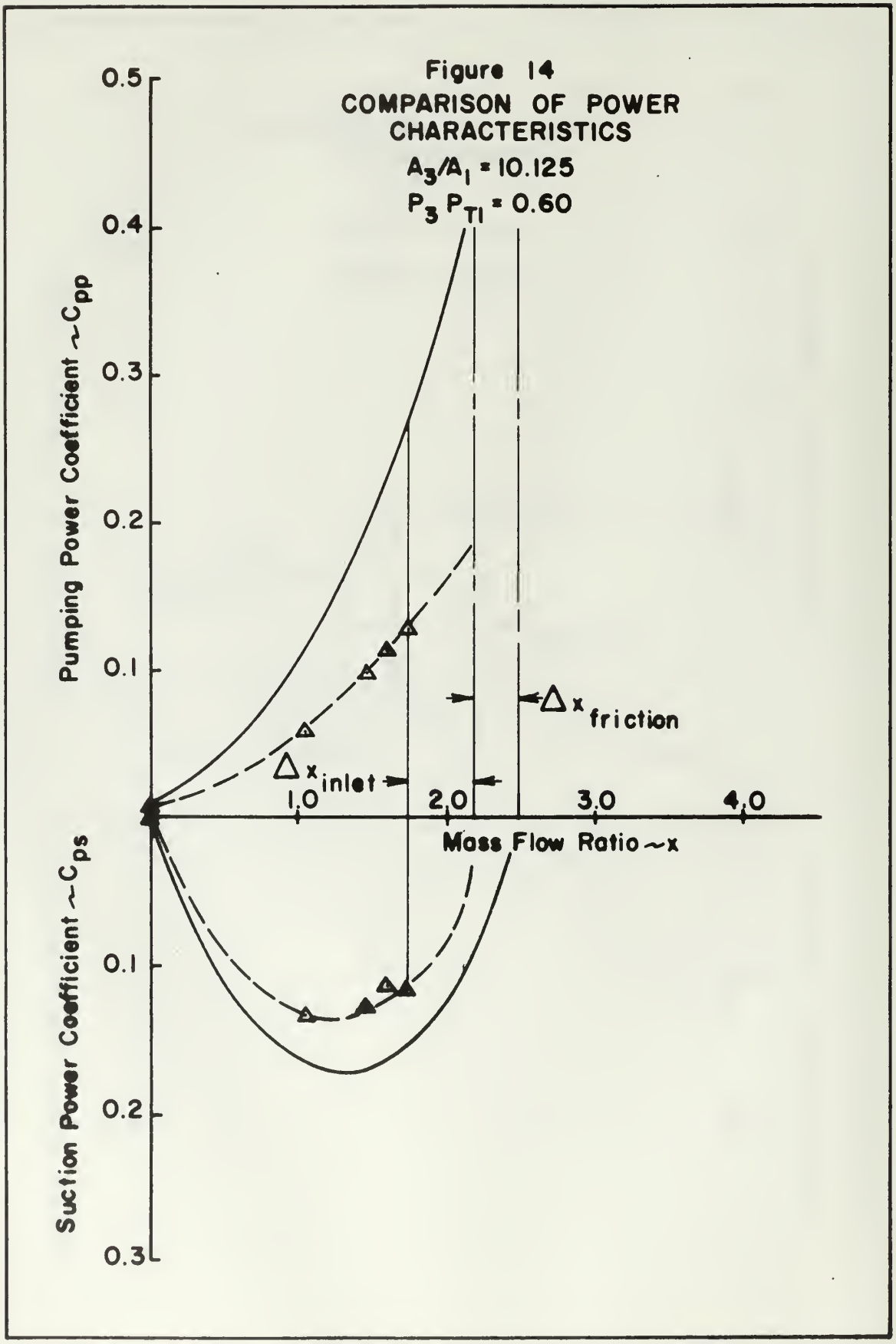
Figure 14
COMPARISON OF POWER CHARACTERISTICS
$A_3/A_1 = 10.125$
$P_3 P_{T1} = 0.60$
0.5
0.4
0.3
0.2
0.1
Pumping Power Coefficient ~ C_{pp}
$\Delta x_{friction}$
Δx_{inlet}
1.0
2.0
3.0
4.0
Mass Flow Ratio ~ x
Suction Power Coefficient ~ C_{ps}
0.1
0.2
0.3

Figure 15
COMPARISON OF PUMPING CHARACTERISTICS

$A_3/A_1 = 10.125$

$P_3/P_{T1} = 0.60$

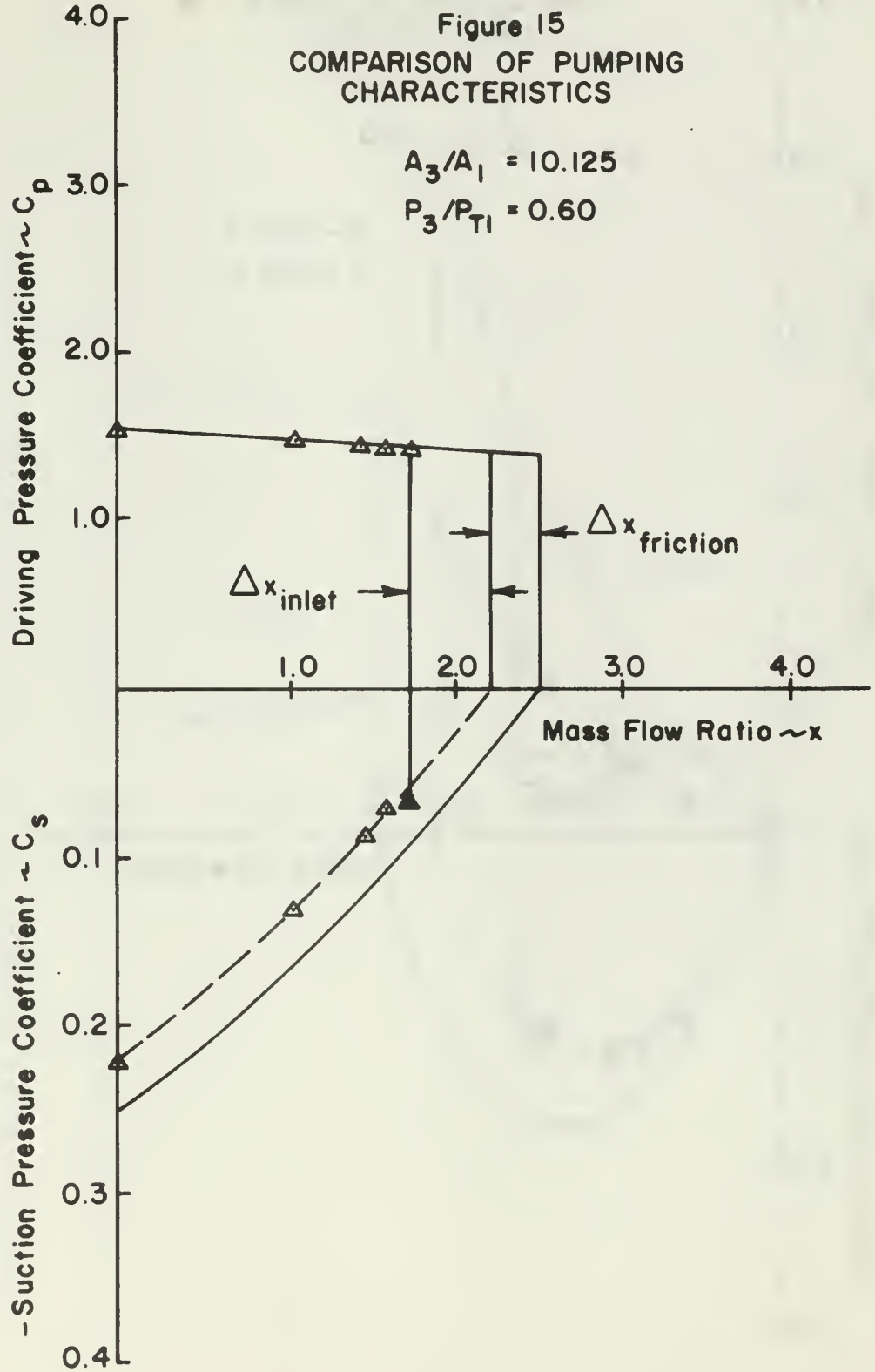

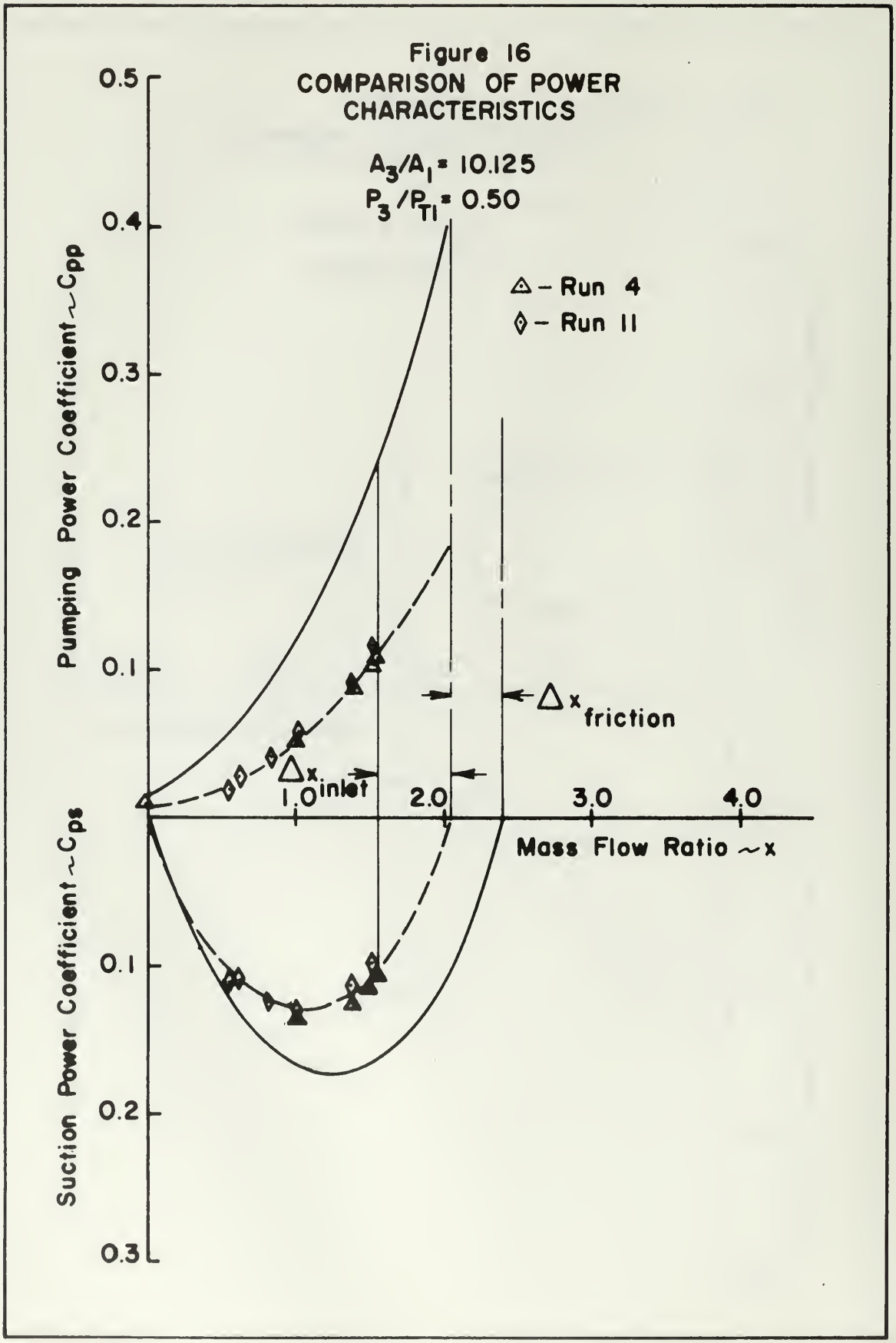
Figure 16
COMPARISON OF POWER CHARACTERISTICS
$A_3/A_1 = 10.125$
$P_3/P_{T1} = 0.50$
Δ – Run 4
◊ – Run 11
Pumping Power Coefficient ~ C_{pp}
Suction Power Coefficient ~ C_{ps}
0.5
0.4
0.3
0.2
0.1
0.1
0.2
0.3
$\Delta x_{friction}$
Δx_{inlet}
1.0
2.0
3.0
4.0
Mass Flow Ratio ~ x

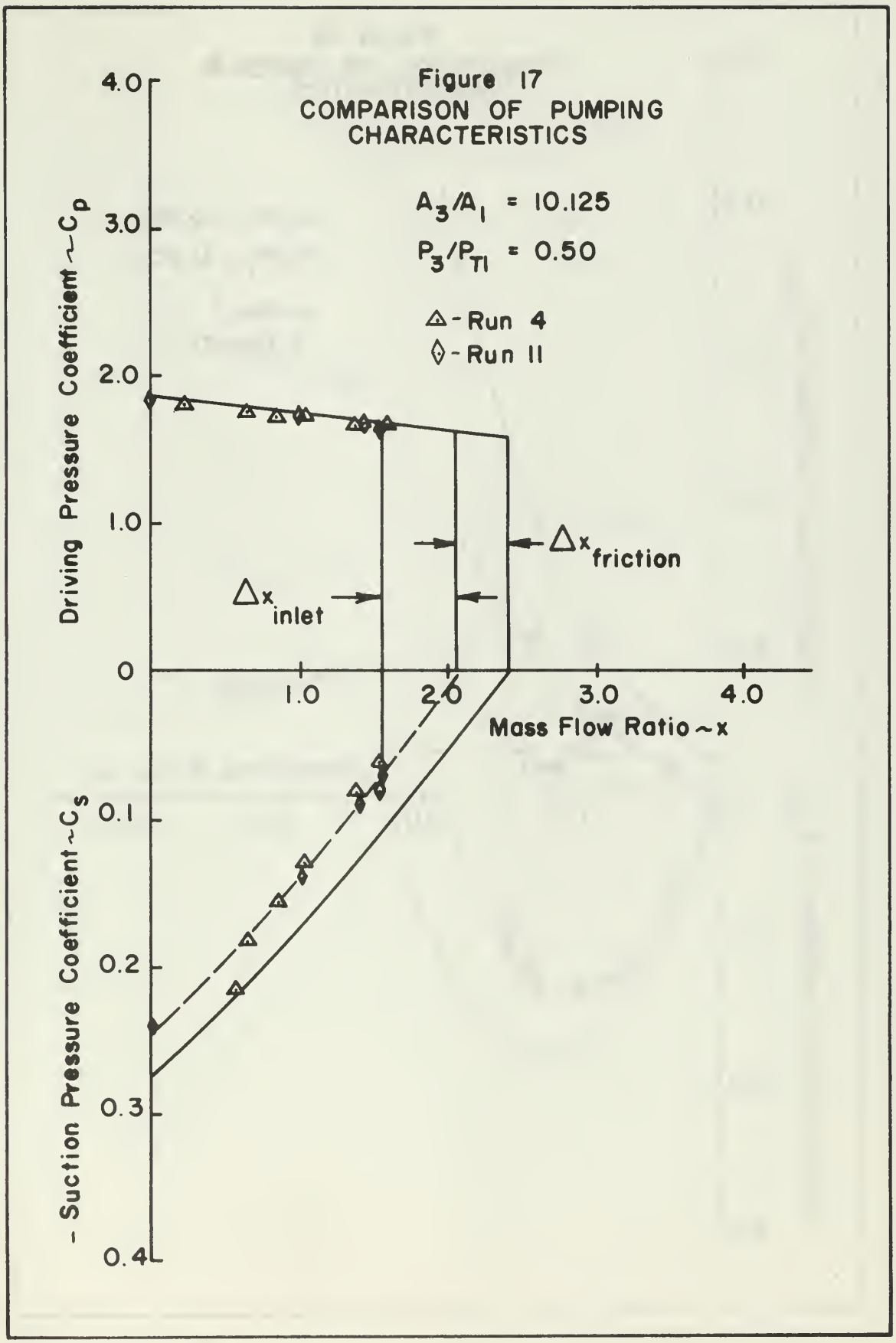
Figure 17
COMPARISON OF PUMPING CHARACTERISTICS
A_3/A_1 = 10.125
P_3/P_{T1} = 0.50
△ - Run 4
◊ - Run 11
Driving Pressure Coefficient ~ C_p
- Suction Pressure Coefficient ~ C_s
Mass Flow Ratio ~ x
Δx_{inlet}
$\Delta x_{friction}$
4.0
3.0
2.0
1.0
0
0.1
0.2
0.3
0.4
1.0
2.0
3.0
4.0

Figure 18
COMPARISON OF POWER CHARACTERISTICS

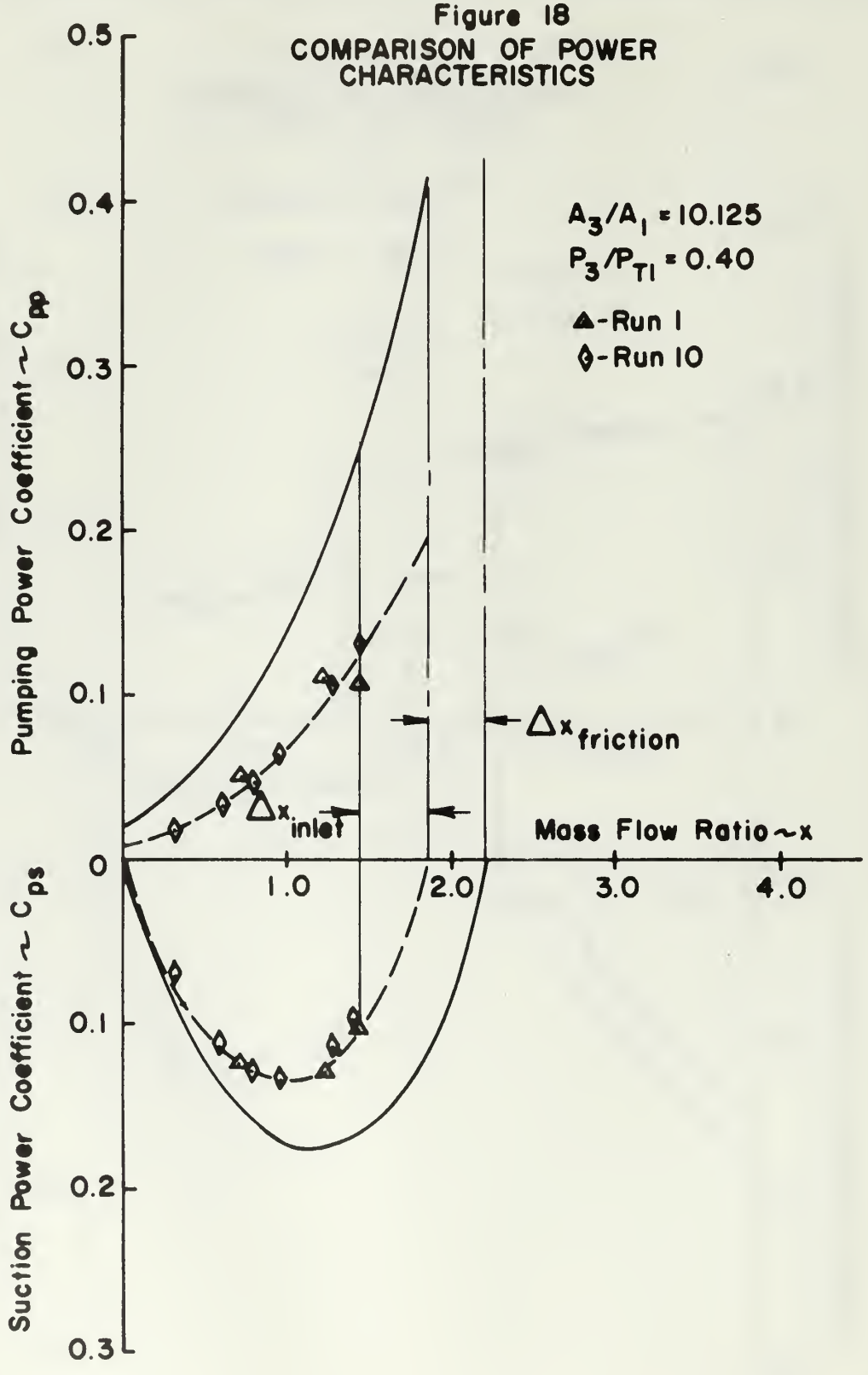

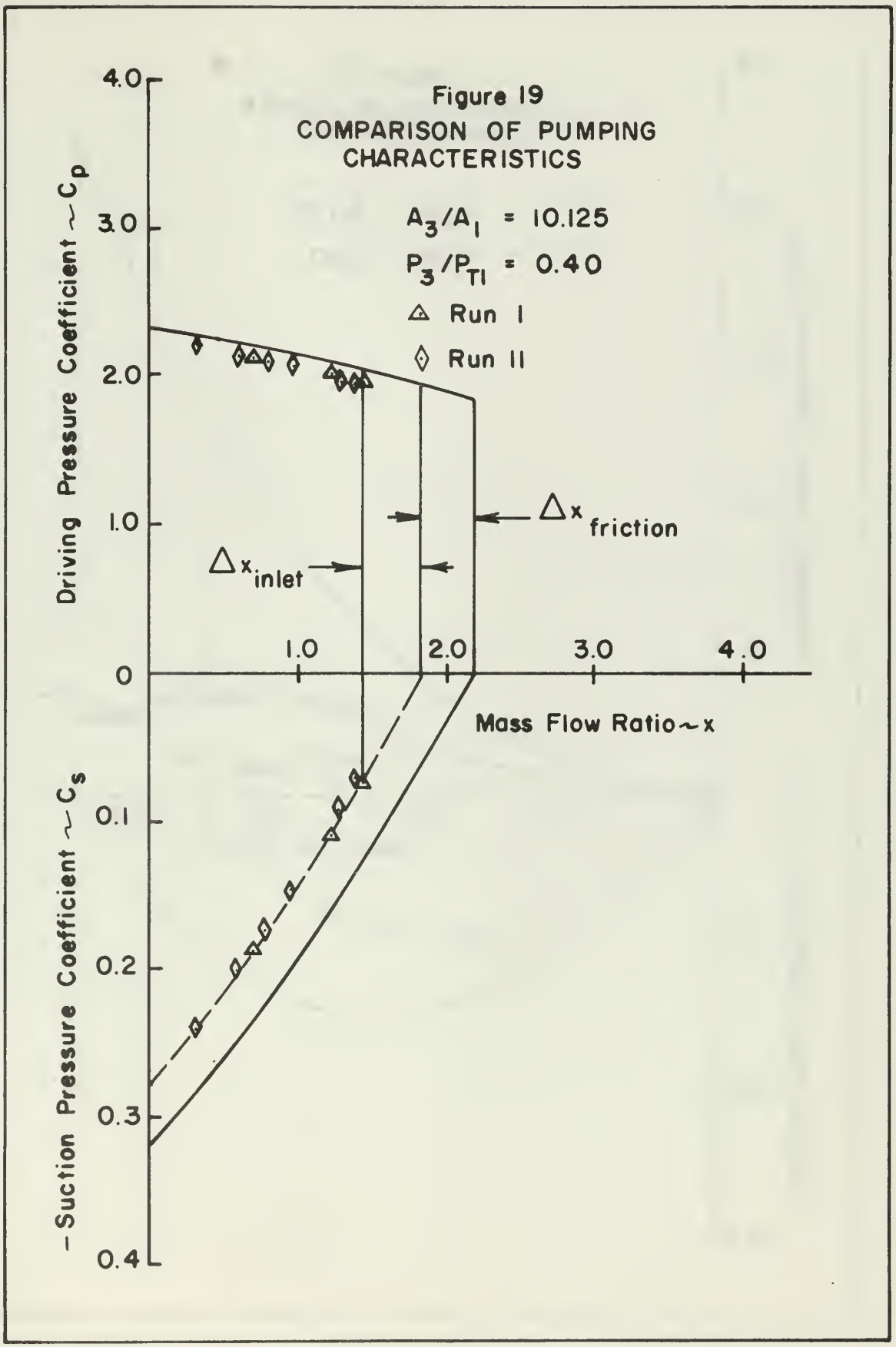
Figure 19
COMPARISON OF PUMPING CHARACTERISTICS
A_3/A_1 = 10.125
P_3/P_{T1} = 0.40
Run I
Run II
$\Delta x_{friction}$
Δx_{inlet}
Driving Pressure Coefficient ~ C_p
- Suction Pressure Coefficient ~ C_s
Mass Flow Ratio ~ x
4.0
3.0
2.0
1.0
0
0.1
0.2
0.3
0.4
1.0
2.0
3.0
4.0

Figure 20

COMPARISON OF POWER CHARACTERISTICS

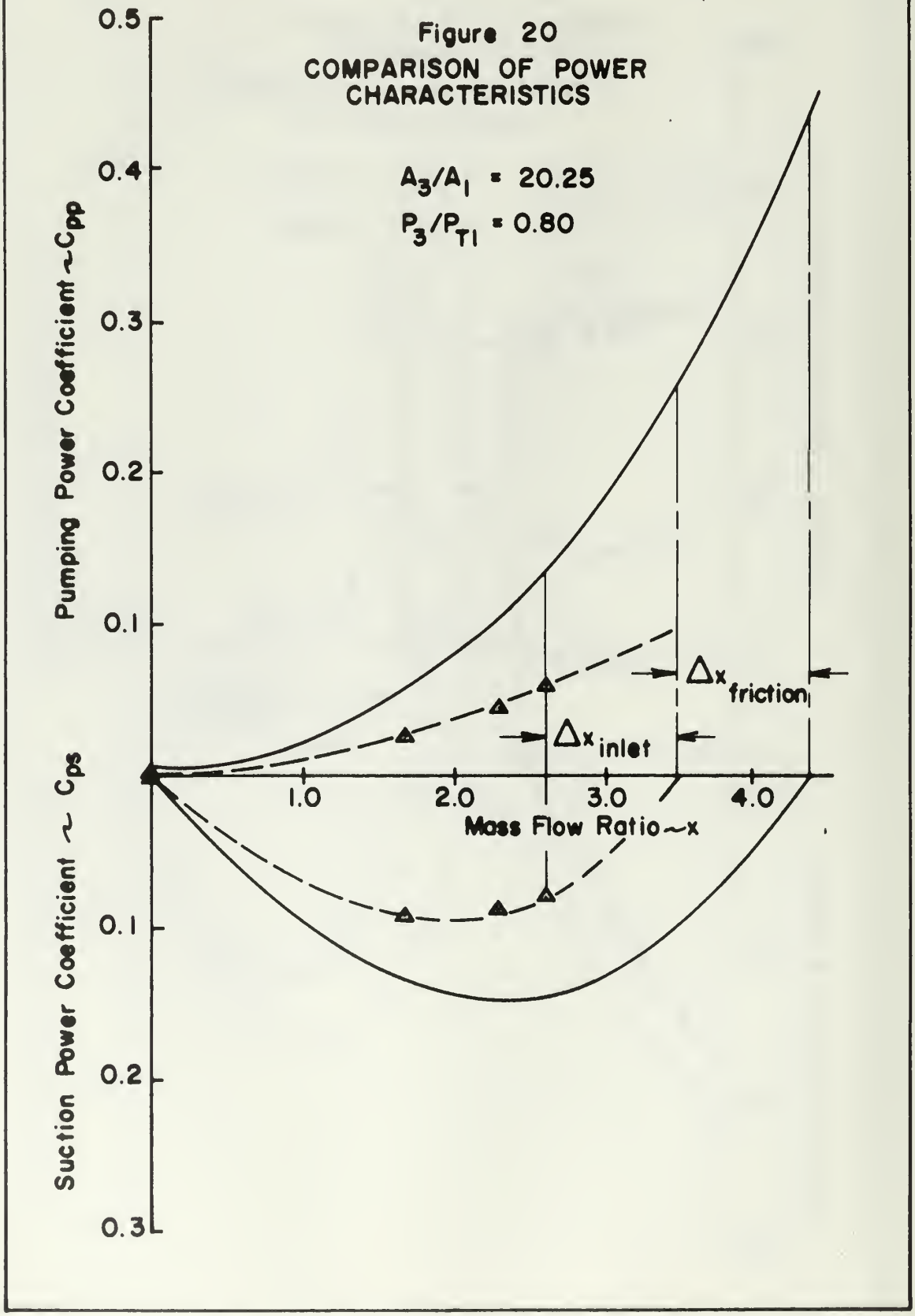

Figure 21
COMPARISON OF PUMPING CHARACTERISTICS

$A_3/A_1 = 20.25$

$P_3/P_{T1} = 0.80$

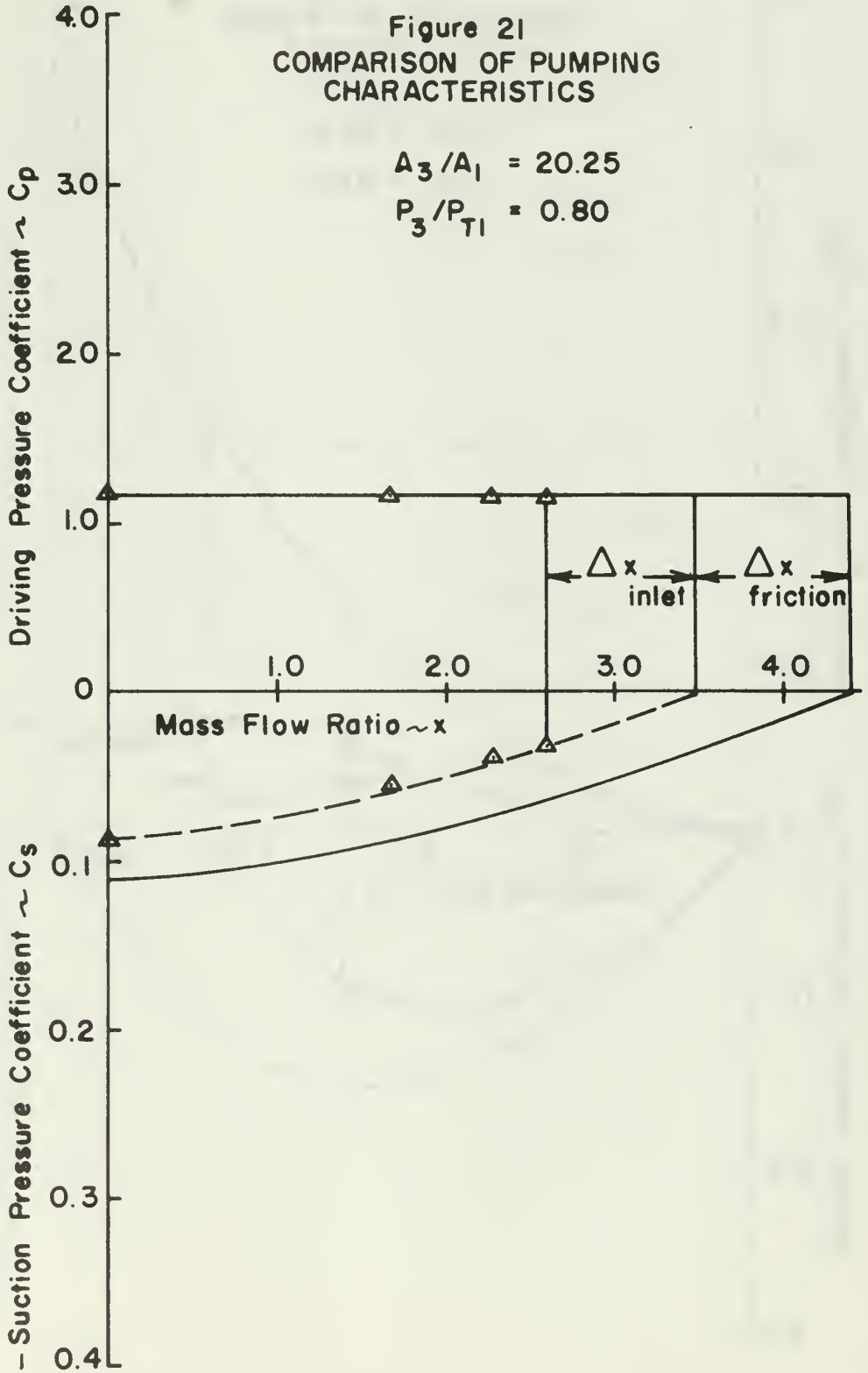

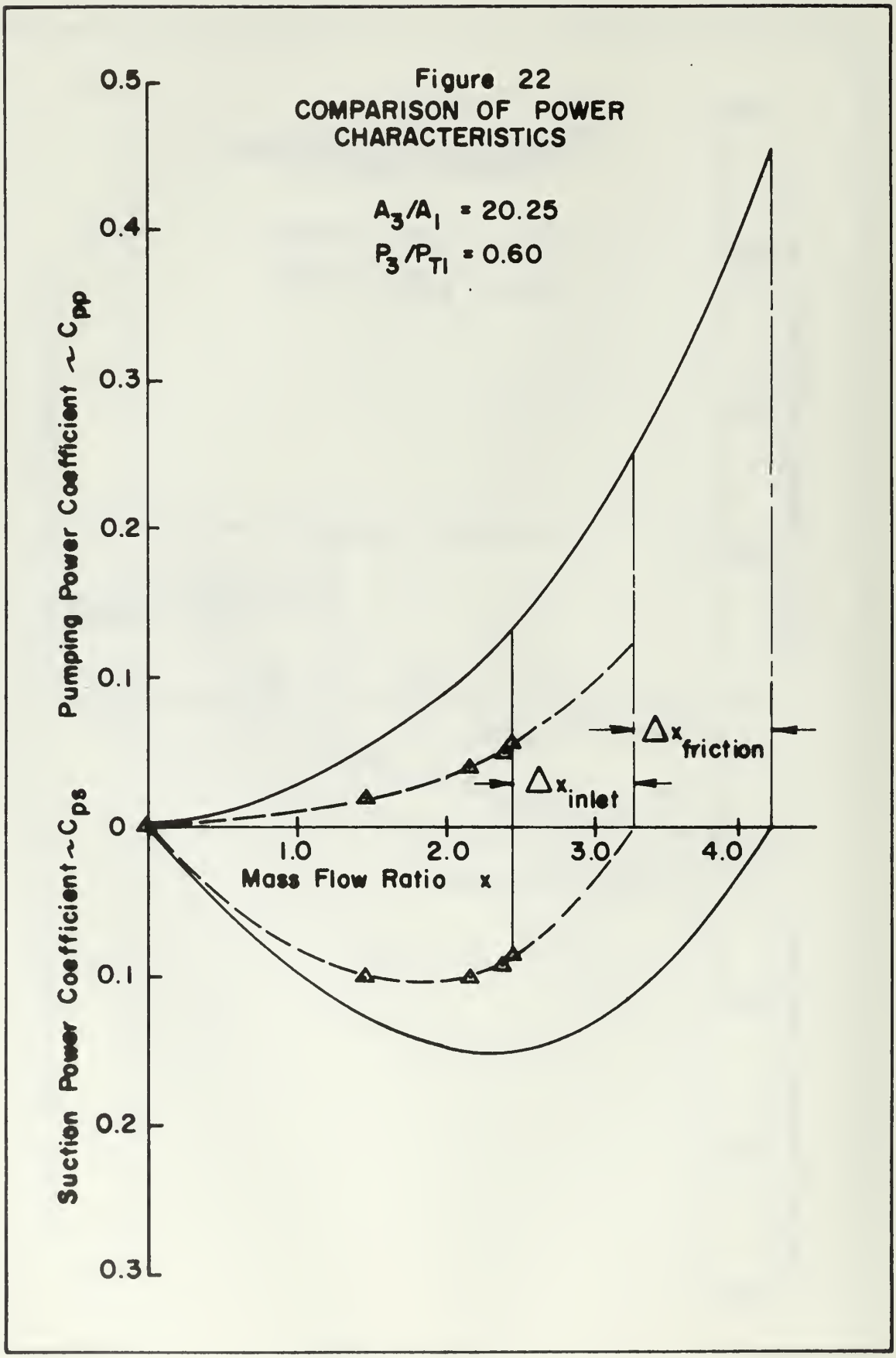
Figure 22
COMPARISON OF POWER CHARACTERISTICS
$A_3/A_1 = 20.25$
$P_3/P_{T1} = 0.60$
0.5
0.4
0.3
0.2
0.1
0
0.1
0.2
0.3
Pumping Power Coefficient ~ C_{pp}
Suction Power Coefficient ~ C_{ps}
1.0
2.0
3.0
4.0
Mass Flow Ratio x
$\Delta x_{friction}$
Δx_{inlet}

Figure 23

COMPARISON OF PUMPING CHARACTERISTICS

$A_3/A_1 = 20.25$

$P_3/P_{T1} = 0.60$

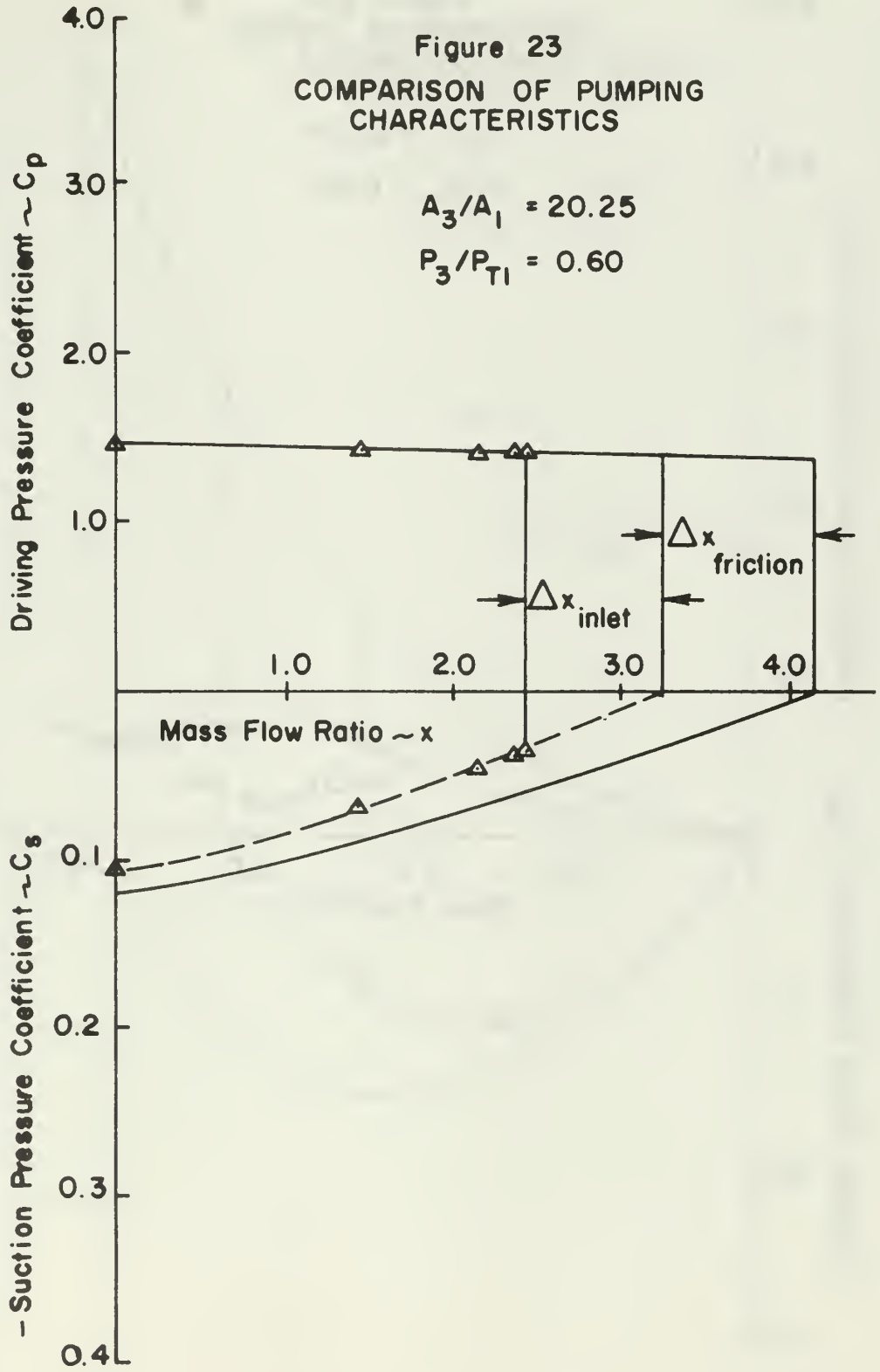

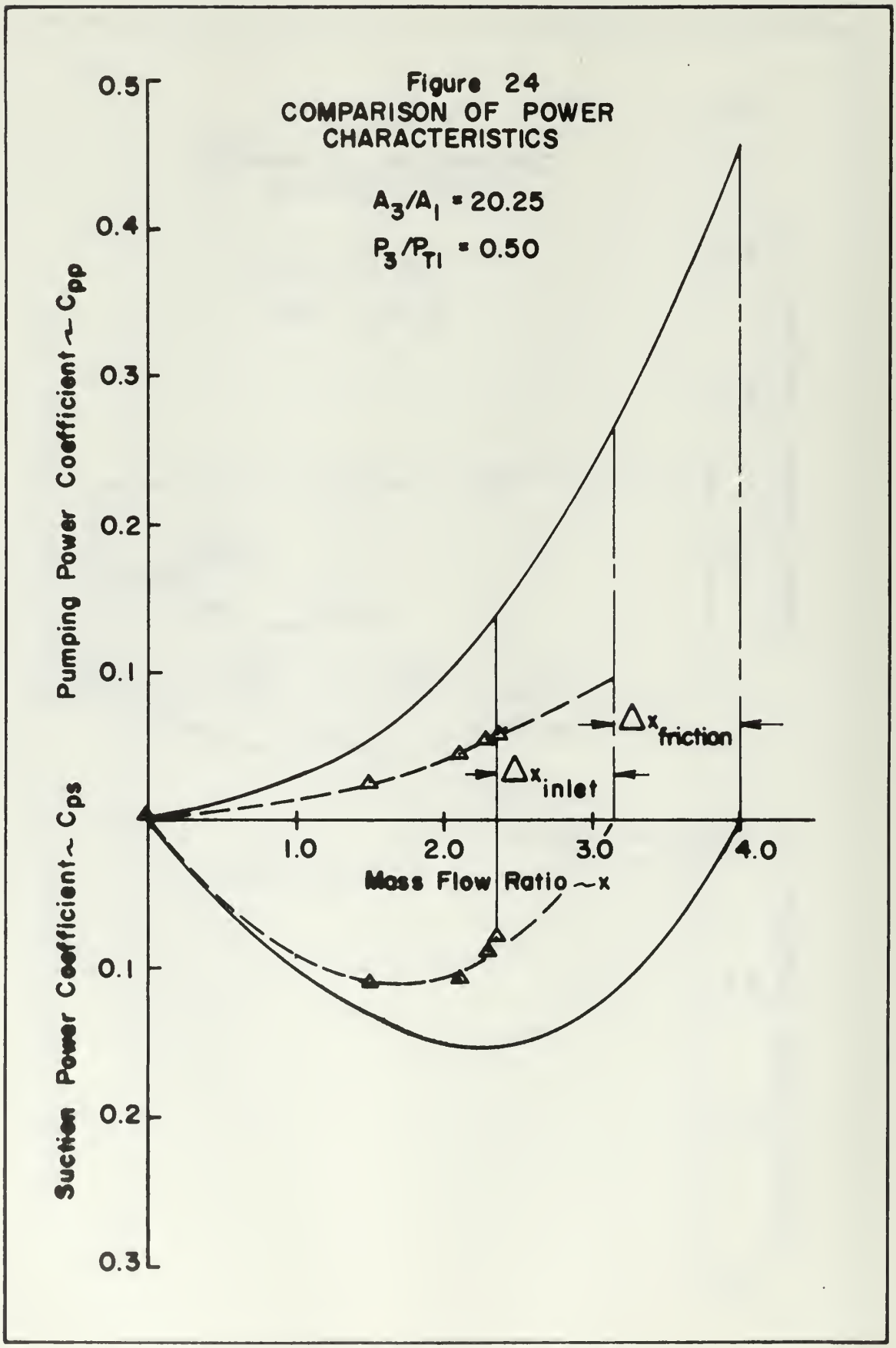
Figure 24
COMPARISON OF POWER CHARACTERISTICS
$A_3/A_1 = 20.25$
$P_3/P_{T1} = 0.50$
Pumping Power Coefficient ~ C_{pp}
Suction Power Coefficient ~ C_{ps}
0.5
0.4
0.3
0.2
0.1
0.1
0.2
0.3
1.0
2.0
3.0
4.0
Mass Flow Ratio ~ x
$\Delta x_{friction}$
Δx_{inlet}

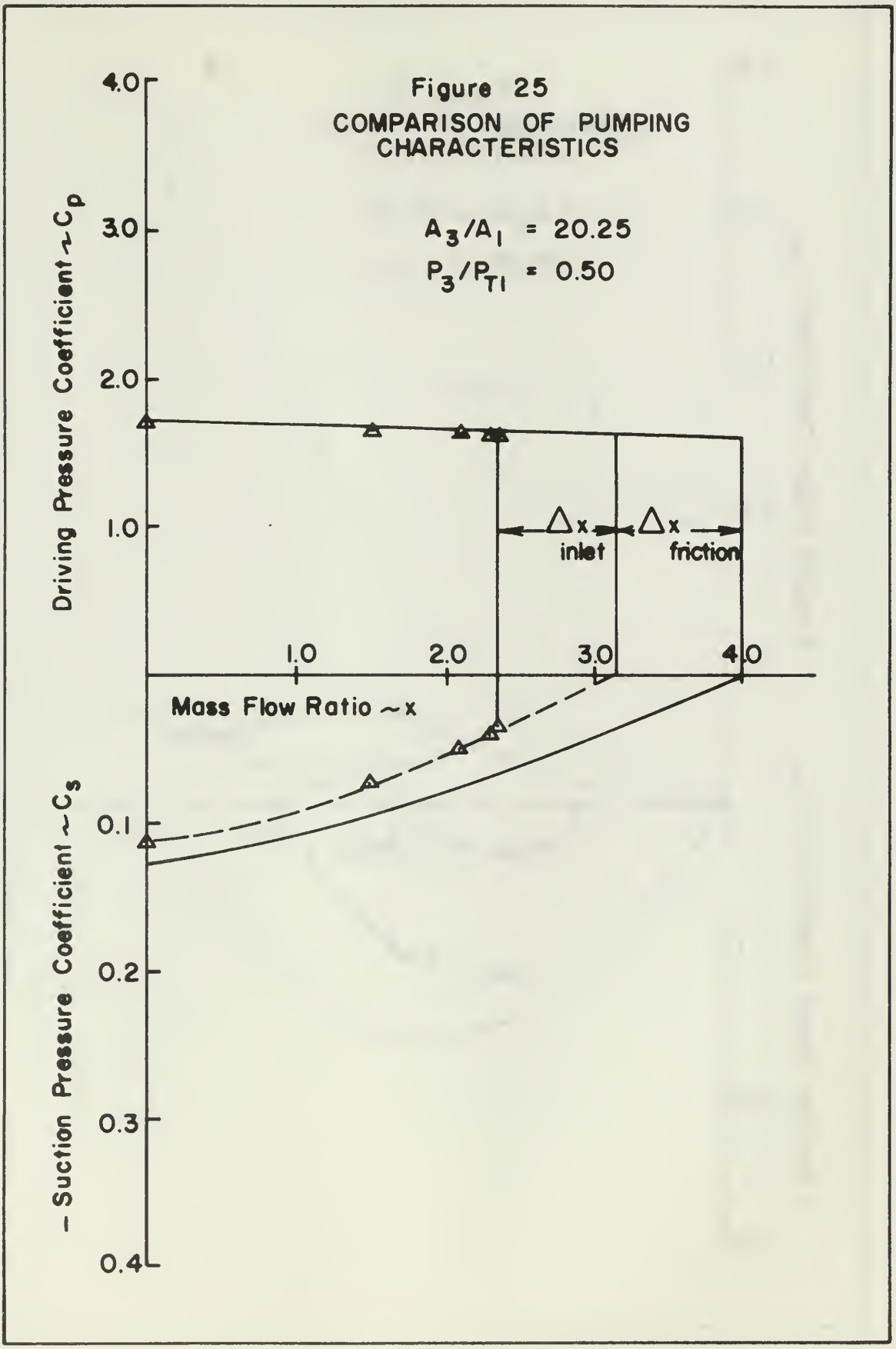
Figure 25
COMPARISON OF PUMPING CHARACTERISTICS
A_3/A_1 = 20.25
P_3/P_{T1} = 0.50
Driving Pressure Coefficient ~ C_p
- Suction Pressure Coefficient ~ C_s
Mass Flow Ratio ~ x
Δx inlet
Δx friction
4.0
3.0
2.0
1.0
0.1
0.2
0.3
0.4
1.0
2.0
3.0
4.0

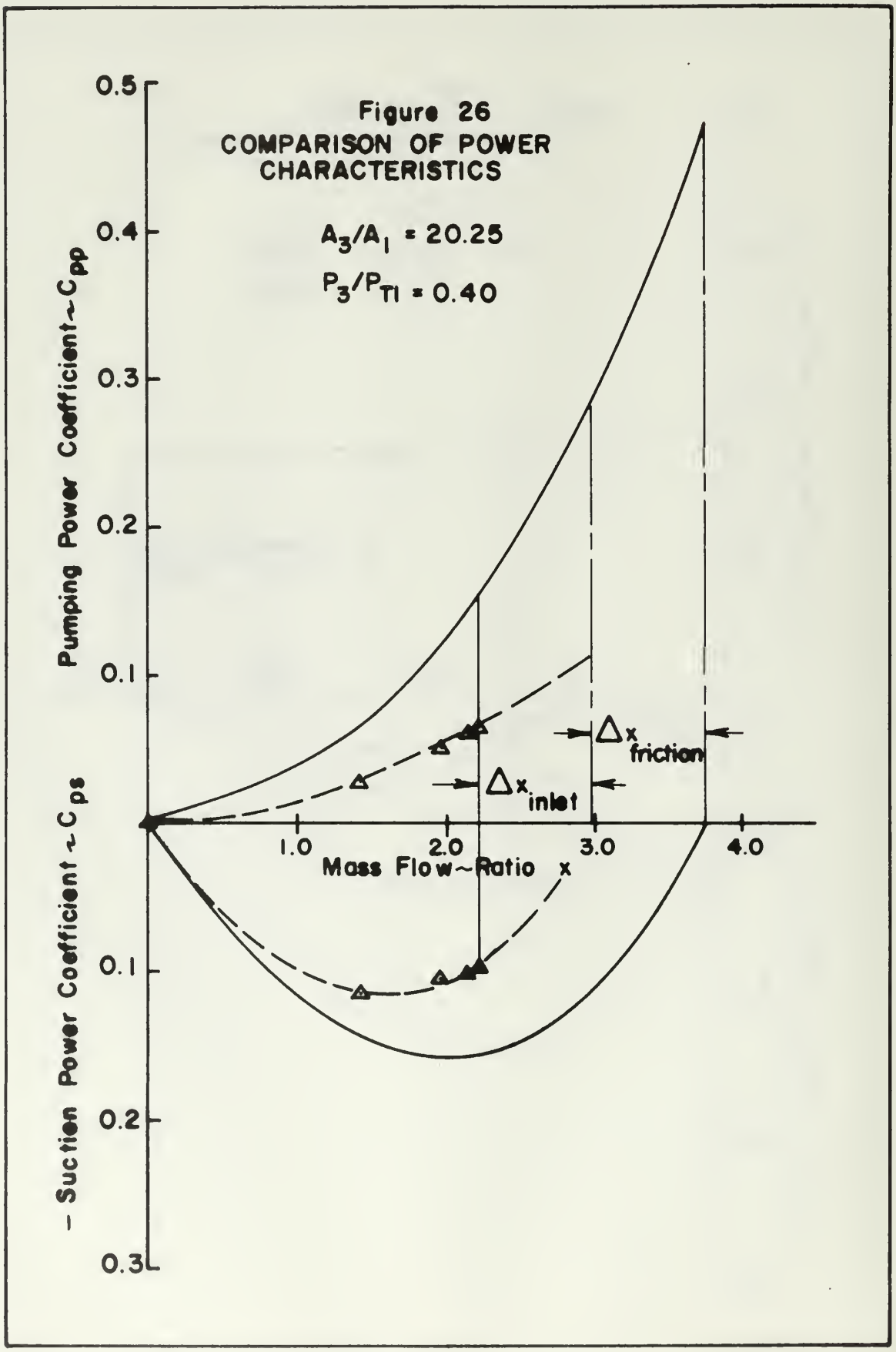
Figure 26
COMPARISON OF POWER CHARACTERISTICS
$A_3/A_1 = 20.25$
$P_3/P_{T1} = 0.40$
Pumping Power Coefficient ~ C_{pp}
- Suction Power Coefficient ~ C_{ps}
0.5
0.4
0.3
0.2
0.1
0.1
0.2
0.3
1.0
2.0
3.0
4.0
Mass Flow ~ Ratio x
$\Delta x_{friction}$
Δx_{inlet}

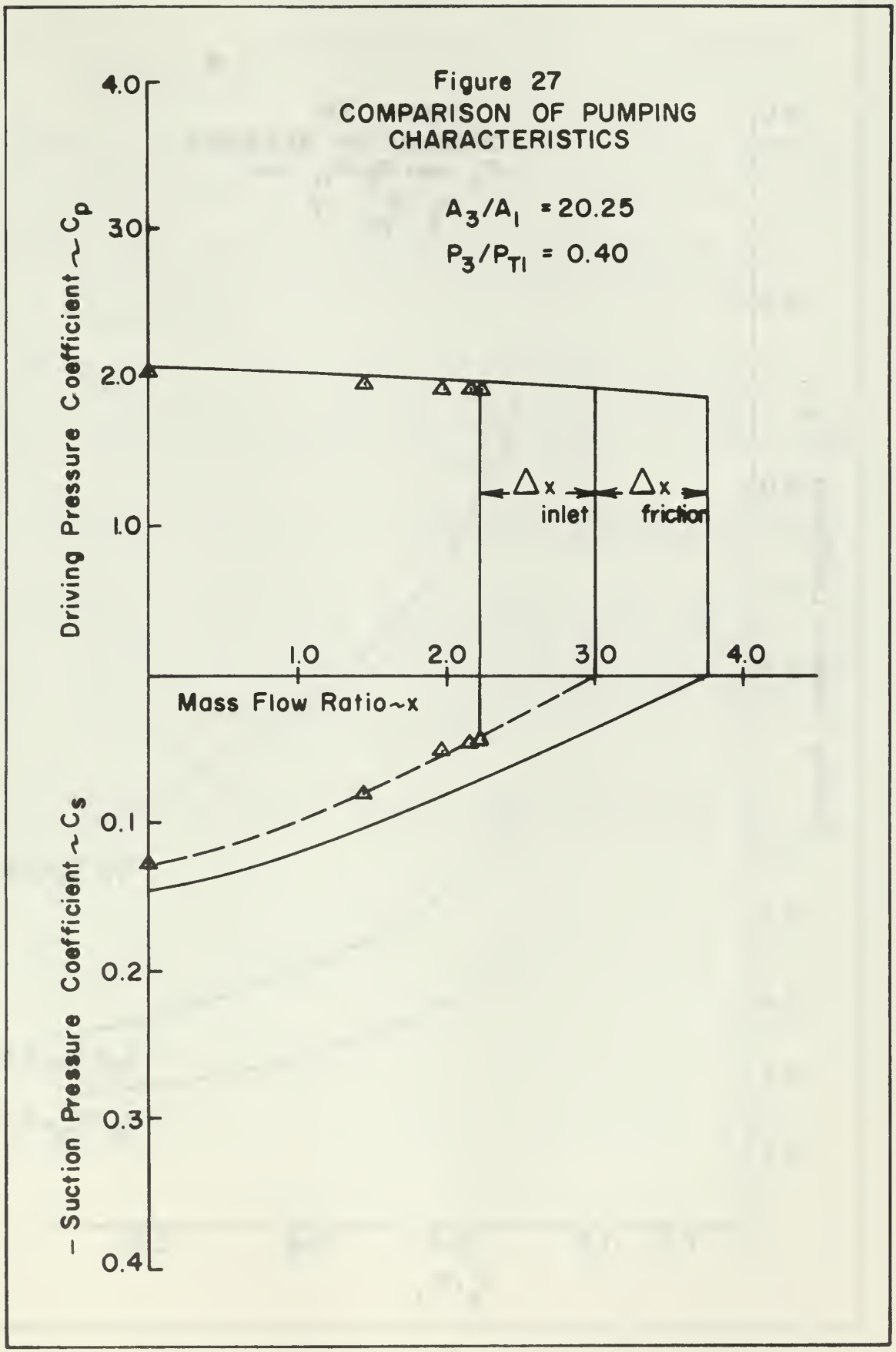
Figure 27
COMPARISON OF PUMPING CHARACTERISTICS
A_3/A_1 = 20.25
P_3/P_{T1} = 0.40
Driving Pressure Coefficient ~ C_p
- Suction Pressure Coefficient ~ C_s
Mass Flow Ratio ~ x
4.0
3.0
2.0
1.0
0.1
0.2
0.3
0.4
1.0
2.0
3.0
4.0
Δx inlet
Δx friction

Figure 28
CORRELATION BETWEEN
C_p and P_3/P_{T1} for
$P_3/P_{T2} = 1.0$

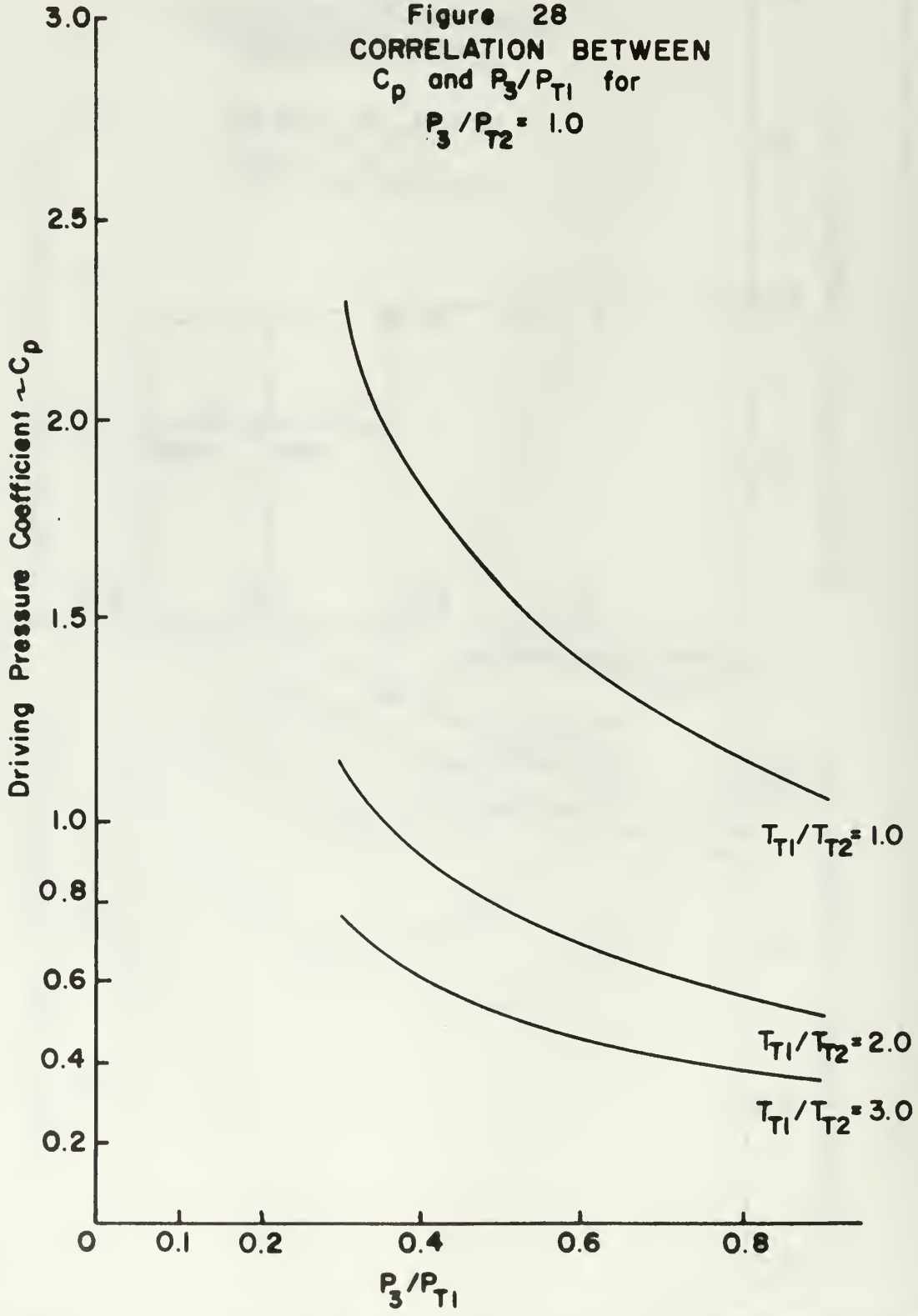

BIBLIOGRAPHY

1. Belter, R. H. Theoretical Performance of the Heated Jet Pump. M.S. Thesis, U. S. Naval Postgraduate School, 1963.

2. Ridder, W. C. and C. R. Summers. Theoretical Analysis of the Heated Jet Pump and Design of a Test Facility. M.S. Thesis, U. S. Naval Postgraduate School, 1966.

3. Wade, B. S. Model Design Study for FAA Nacelle Fire Tests in 3W Test Cell. U. S. Naval Air Turbine Test Station, Aeronautical Turbine Laboratory, August 1963.

4. Vavra, M. H. Determination of Flow Rates of Allis-Chalmers Axial Flow Compressor VA-312 of Propulsion Laboratories by Means of Square-Edged Orifices, U. S. Naval Postgraduate School, Department of Aeronautics, Technical Note 63T-2, November 1963.

5. Stearnes, R. F., et al. Flow Measurement with Orifice Meters. Van Nostrand Co., Inc., New York, 1951.

6. Lockwood, R. M., and W. G. Patterson. Interim Summary Report Covering the Period from 1 April 1961 to 30 June 1962 on Investigation of the Process of Energy Transfer from an Intermittent Jet to Secondary Fluid in an Ejector-type Thrust Augmenter, Report No. ARD-305, Advanced Research Division of Hiller Aircraft Company, June 1962.

7. Haroldsen, O. O. Ejector Model Test Program for J-2 Altitude System. Report R5699, Rocketdyne, May 1964.

APPENDIX A

Theoretical Analysis

1. Dimensional Analysis

For a thermodynamic system, in which electrical effects are insignificant, there are four basic dimensions which describe the system. According to the Buckingham Pi Theorem, these four dimensions serve as a base by which all physical characteristics can be non-dimensionalized.

Choosing force, length, time, and temperature as the base dimensions, the following physical parameters were chosen to collectively represent these base dimensions.

a. Secondary ambient density -- ρ_{T2}

b. Secondary ambient temperature -- T_{T2}

c. Primary mass flow rate -- $\dot{m}_1$

d. Primary available enthalpy -- H_a

With these reference parameters, it is possible to non-dimensionalize any physical quantity in a thermodynamic system.

Consider, for a given output power P, a non-dimensional power coefficient C_p, obtained in the following manner:

Power - units of $\frac{FL}{T}$

Therefore, to obtain a power coefficient based upon the selected reference parameters:

ρ_{T2} - $\frac{FT^2}{L^4}$

T_{T2} - Θ

H_a - $\frac{L^2}{T^2}$

$\dot{m}_1$ - $\frac{FT}{L}$

Define

$$C_p - \frac{P\left(\frac{FL}{T}\right)}{\rho_{T2}{}^a \; T_{T2}{}^b \; H_a{}^c \; \dot{m}_1{}^d} \qquad \text{(A-1)}$$

setting up four equations to solve for a, b, c, d.

$$C_p - \frac{(FL/T)}{\left(\frac{FT^2}{L^4}\right)^a \; \Theta^b \; \left(\frac{L^2}{T^2}\right)^c \; \left(\frac{FT}{L}\right)^d} \qquad \text{(A-2)}$$

F: $a + d = 1$ (A-3)

L: $-4a + 2_c - d = 1$ (A-4)

T: $2a - 2_c + d = -1$ (A-5)

Θ: $b = 0$ (A-6)

adding equations A-4 and A-5

$$-2_a = 0$$

or

$$a = 0 \qquad \text{(A-7)}$$

therefore, from equation A-3

$$d = 1 \qquad \text{(A-8)}$$

now from equation A-5

$$-2a + 1 = -1$$

or

$$c = 1 \qquad \text{(A-9)}$$

$$C_p = \frac{\text{Power}}{\dot{m}_1 \; H_a} \qquad \text{(A-10)}$$

In this manner it is possible to define any number of dimensionless coefficients.

2. Definition of Performance Coefficients

Referring to Figure 1, the following parameters are obtained:

$$H_a = C_p (T_{T1} - T_3^1) \tag{A-11}$$

$$H_a = C_p T_{T1} \left(1 - \left(\frac{P_3}{P_{T1}}\right)^{\frac{\gamma-1}{\gamma}}\right) \tag{A-12}$$

similarly,

$$H_3 = C_p T_{T3} \left[1 - \left(\frac{P_3}{P_{T3}}\right)^{\frac{\gamma-1}{\gamma}}\right] \tag{A-13}$$

From the 1st and 2nd Laws of Thermodynamics,

$$dh = TdS + V_{dp} \tag{A-14}$$

for the isothermal compression from state i to state T_2,

$$dh = 0 \tag{A-15}$$

therefore,

$$ds_{i \to T2} = -\frac{v}{T} dp_{i \to T2} \tag{A-16}$$

for a perfect gas, the incremental change in entropy from i to T2 can be defined as:

$$\Delta S_{i \to T2} = -R_{\ell n} \frac{P_{T2}}{P_i} = R_{\ell n} \frac{P_3}{P_{T2}} \tag{A-17}$$

The equivalent work done by the isothermal compression is therefore

$$H_s = RT_{T2} \ell n \frac{P_3}{P_{T2}} \tag{A-18}$$

With these enthalpies defined, it is now possible to develop the power output coefficients for an ejector.

The power available at the exit from the mixing section is defined as the pumping power and therefore the pumping power coefficient can be defined as:

$$C_{pp} = \frac{(\dot{m}_1 + \dot{m}_2)\, H_3}{\dot{m}_1\, H_a} \qquad \text{(A-19)}$$

or substituting equations A-12 and A-13,

$$C_{pp} = \left(\frac{\dot{m}_1 + \dot{m}_2}{\dot{m}_1}\right) \left(\frac{T_{T3}}{T_{T1}}\right) \left[\frac{1 - \left(P_3/P_{T3}\right)^{\frac{\gamma-1}{\gamma}}}{1 - \left(P_3/P_{T1}\right)^{\frac{\gamma-1}{\gamma}}}\right] \qquad \text{(A-20)}$$

The equivalent work done during the isothermal compression of the secondary fluid is defined as the suction power, and therefore the suction power coefficient is defined as:

$$C_{ps} = \frac{\dot{m}_2\, H_s}{\dot{m}_1\, H_a} \qquad \text{(A-21)}$$

from equations A-12 and A-18

$$C_{ps} = \left(\frac{\dot{m}_2}{\dot{m}_1}\right)\left(\frac{\gamma-1}{\gamma}\right) \left(\frac{T_{T2}}{T_{T1}}\right) \left[\frac{\ell n\ P_3/P_{T2}}{1 - (P_3/P_{T1})^{\frac{\gamma-1}{\gamma}}}\right] \qquad \text{(A-22)}$$

The ratio $\frac{\dot{m}_2}{\dot{m}_1}$ is defined as the non-dimensional mass flow ratio, x. It is also possible to suitably non-dimensionalize the output momentum to obtain the output momentum coefficient.

$$C_M = \left(\frac{\dot{m}_1 + \dot{m}_2}{\dot{m}_1}\right) \frac{V_3}{\sqrt{H_a}} \qquad \text{(A-23)}$$

or

$$C_M = (1 + x)\sqrt{\frac{2H_3}{H_a}}$$

$$C_M = (1 + x) \left\{ \left(\frac{T_{T3}}{T_{T1}} \right) \left[\frac{1 - (P_3/P_{T3})^{\frac{\gamma-1}{\gamma}}}{1 - (P_3/P_{T1})^{\frac{\gamma-1}{\gamma}}} \right] \right\}^{1/2} \quad \text{(A-24)}$$

Recalling the definition of C_{pp},

$$C_M = (1 + x)^{1/2} \, C_{pp}{}^{1/2} \quad \text{(A-25)}$$

These coefficients describe the performance of an ejector as an energy or momentum producing device. Since an ejector is essentially a pump, it becomes necessary to develop certain coefficients which describe the pumping characteristics.

The driving pressure coefficient C_p is defined as:

$$C_p = \frac{P_{T1} - P_3}{\rho_{T2} \, H_a} \quad \text{(A-26)}$$

or, for an ideal gas,

$$C_p = \left(\frac{\gamma-1}{\gamma} \right) \left(\frac{T_{T2}}{T_{T1}} \right) \left(\frac{P_{T1}}{P_{T2}} \right) \left[\frac{1 - P_3/P_{T1}}{1 - (P_3/P_{T1})^{\frac{\gamma-1}{\gamma}}} \right] \quad \text{(A-27)}$$

The suction pressure coefficient is similarly defined.

$$C_s = \frac{P_{T2} - P_3}{\rho_{T2} \, H_a} \quad \text{(A-28)}$$

or

$$C_s = \left(\frac{\gamma-1}{\gamma} \right) \left(\frac{T_{T2}}{T_{T1}} \right) \left[\frac{1 - P_3/P_{T2}}{1 - (P_3/P_{T1})^{\frac{\gamma-1}{\gamma}}} \right] \quad \text{(A-29}$$

The geometric characteristics on an ejector may also be non-dimensionalized in the same manner. Consider the cross sectional area of the mixing section A_3, then

$$C_{A3} = \frac{A_3}{\rho_{T2}{}^a \, T_{T2}{}^b \, \dot{m}_1{}^c \, H_a{}^d} \tag{A-30}$$

Setting up the four dimensional unit equations yields,

$$A_3(L^2) = \left(\frac{FT^2}{L^4}\right)^a \theta^b \left(\frac{FT}{L}\right)^c \left(\frac{L^2}{T^2}\right)^d \tag{A-31}$$

or

$$L: \quad 2 = -4a - c + 2d \tag{A-32}$$

$$F: \quad o = a + c \tag{A-33}$$

$$T: \quad 0 = 2a + c - 2d \tag{A-34}$$

$$\theta: \quad 0 = b \tag{A-35}$$

adding A-32 and A-34 gives

$$2 = -2a$$

$$\therefore a = -1$$

$$\therefore c = +1$$

$$b = o$$

$$d = -1/2$$

thus,

$$C_{A3} = A_3 \left(\frac{\rho_{T2}}{\dot{m}_1}\right)\sqrt{H_a} \tag{A-36}$$

It was found that the actual controlling geometric parameters could be expressed by an area coefficient and the ratio of A_3 to the primary nozzle area A_1. Thus,

$$K^2 \triangleq \frac{A_3}{A_1} \tag{A-37}$$

was used for the non-dimensional area parameter along with C_{A3}.

3. Detailed Development

Consider the mixing of two concentric jets in a constant area, frictionless duct.

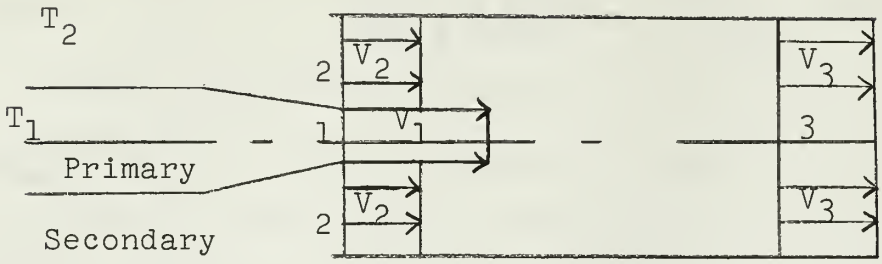

Nomenclature

AREAS

A_1 = Primary area

A_2 = Secondary area

A_3 = Mixing section area

introduce non-dimensional area ratio, K^2, thus,

$$A_2 = (K^2 - 1)\, A_1$$

$$A_3 = K^2\, A_1$$

MASS FLOW RATES

$\dot{m}_1$ = Primary mass flow rate

$\dot{m}_2$ = Secondary flow rate

$\dot{m}_3$ = Total flow rate

recalling definition of $x = \frac{\dot{m}_2}{\dot{m}_1}$;

$$\dot{m}_2 = x\, \dot{m}_1$$

DENSITIES

ρ_1 = Primary density

ρ_2 = Secondary density

ρ_3 = Exit density

let

$$\delta = \frac{\rho_2}{\rho_1}$$

VELOCITIES

V_1 = Primary velocity at exit from nozzle

V_2 = Secondary velocity at exit from nozzle

V_3 = Final velocity

let

$$r = \frac{V_2}{V_1}$$

From the definition of mass flow rate,

$$x = \frac{\dot{m}_2}{\dot{m}_1} = \frac{\rho_2 A_2 V_2}{\rho_1 A_1 V_1} \qquad \text{(A-38)}$$

or finally,

$$x = \delta(K^2 - 1)\, r \qquad \text{(A-39)}$$

from continuity,

$$\dot{m}_3 = \dot{m}_1 + \dot{m}_2 \qquad \text{(A-40)}$$

$$\rho_3 A_3 V_3 = \rho_1 A_1 V_1 + \rho_2 A_2 V_2$$

$$\left(\frac{\rho_3}{\rho_1}\right) K^2 \left(\frac{V_3}{V_1}\right) = (1 + x)$$

therefore,

$$\frac{\rho_3}{\rho_1} = \frac{(1 + x)}{K^2} \left(\frac{V_1}{V_3}\right) \qquad \text{(A-41)}$$

Now, consider the constant pressure mixing of two ideal gases in a constant area duct.

$$\dot{m}_1 C_p T_1 + \dot{m}_2 C_p T_2 = \dot{m}_3 C_p T_3$$

or

$$\frac{C_p P_1}{\rho_1 R} + \frac{x C_p P_2}{P_2 R} = (1 + x) \frac{C_p P_3}{\rho_3 R}$$

for air $\frac{C_p}{R} = \frac{\gamma - 1}{\gamma}$ = constant

therefore,

$$\frac{P_1}{\rho_1} + \frac{x P_2}{\rho_2} = (1 + x) \frac{P_3}{\rho_3}$$

but $P_1 = P_2 = P_3$

thus,

$$\left(\frac{P_1}{\rho_3}\right) = \frac{(1 + x/\delta)}{(1 + x)} \qquad \text{(A-42)}$$

As a comparison, consider the mixing of two liquids at constant volume,

$$\frac{\dot{m}_1}{\rho_1} + \frac{\dot{m}_2}{\rho_2} = \frac{\dot{m}_3}{\rho_3}$$

or

$$\left(\frac{\rho_1}{\rho_3}\right) = \frac{(1 + x/\delta)}{(1 + x)} \qquad \text{(A-43)}$$

Now assume that the actual mixing process can be described in a similar manner such that the compressibility effects are taken into account by some change in volume of the primary fluid. By introducing a compressibility factor μ, the mixing process can be described by

$$\frac{\rho_1}{\rho_3} = \frac{(\mu + x/\delta)}{(1 + x)} \qquad \text{(A-44)}$$

The value of μ will be unity for the case of incompressible mixing. For the compressible case, μ can be determined from energy considerations as will be shown later.

Rewriting equation A-44

$$\frac{\rho_3}{\rho_1} = \frac{(1 + x)}{(\mu + x/\delta)}$$

Combining this result with equation A-41,

$$\frac{\rho_3}{\rho_1} = \frac{(1 + x)}{(\mu + x/\delta)} = \frac{(1 + x)}{K^2}\left(\frac{V_1}{V_3}\right)$$

therefore,

$$\left(\frac{V_3}{V_1}\right) = \frac{(\mu + x/\delta)}{K^2} \qquad \text{(A-45)}$$

Now, apply the momentum equation for the case of a frictionless mixing section with uniform velocity distributions.

$$P_1 A_1 + P_2 A_2 - P_3 A_3 = \dot{m}_3 V_3 - \dot{m}_1 V_1 - \dot{m}_2 V_2$$

dividing thru by ρ_1 and A_1 yields

$$\frac{P_1}{\rho_1} + \frac{P_2}{\rho_1}(K^2-1) - \frac{P_3}{\rho_1}K^2 = \left(\frac{P_3}{\rho_1}\right) K^2 V_3^2 - V_1^2 - \delta(K^2-1)V_2^2 \qquad \text{(A-46)}$$

after substituting for $\left(\frac{\rho_3}{\rho_1}\right)$; $\left(\frac{V_2}{V_1}\right)$; $\left(\frac{V_3}{V_1}\right)$; the following expression is obtained:

$$\frac{P_1}{\rho_1} + \frac{P_2}{\rho_1}(K^2-1) - \frac{P_3}{\rho_1}K^2 = \left[\frac{(1 + x)(\mu + x/\delta)}{K^2} - \frac{x^2}{\delta(K^2-1)}-1\right] V_1^2 \qquad \text{(A-47)}$$

Now, consider

$$P_1 - P_2 = \Delta P_1$$

when

$$M_1 \geq 1$$

or

$$P_1 = P_2 + \Delta P_1$$

thus, looking at the left-hand side of equation A-47,

$$\frac{P_2 + \Delta P_1}{\rho_1} + \frac{P_2(K^2 - 1)}{\rho_1} - \frac{P_3}{\rho_1} K^2 = [\quad] V_1^2$$

or rearranging,

$$\frac{P_3 - P_2}{\rho_1 V_1^2} = - [\quad] - \frac{\Delta P_1}{\rho_1 V_1^2} \qquad \text{(A-48)}$$

Define a non-dimensional pressure rise across the mixing section.

$$\Phi \triangleq \frac{P_3 - P_2}{\rho_2 V_1^2} = \frac{1}{K^2}\left[\frac{1}{\delta} + \frac{\Delta P_1}{\rho_2 V_1^2} + \frac{x^2}{\delta^2(K^2-1)} - \frac{(1+x)(\mu\delta+x)}{\delta^2 K^2}\right] \qquad \text{(A-49)}$$

With this result, along with the definition of μ, it is possible to obtain an interation solution to the mixing problem for any given set of known parameters.

Consider the following known parameters:

1. P_3 = Pamb - fixed value
2. P_{T1} = Controllable value
3. P_{T2} = Controllable value
4. T_{T2}/T_{T1} = Temperature ratio can be controlled
5. K^2 = Known for any given ejector

Now, for a specified value of each of these parameters, the following technique was employed to obtain a solution:

a. Assume a value of M_2.

b. For $M_1 \leq 1$, calculate M_1.

$$\frac{P_{T1}}{P_1} = \left[1 + \frac{\gamma-1}{2} M_1^2\right]^{\gamma/\gamma-1}$$

or

$$M_1^2 = \left(\frac{2}{\gamma-1}\right)\left[\left(\frac{P_{T1}}{P_1}\right)^{\frac{\gamma-1}{\gamma}} - 1\right]$$

but

$$\frac{P_2}{P_{T2}} = \frac{1}{\left[1 + \frac{\gamma-1}{2} M_2^2\right]}^{\gamma/\gamma-1}$$

therefore, for $M_1 < 1$, $P_2 = P_1$

and

$$M_1^2 = \left(\frac{2}{\gamma-1}\right)\left\{\left(\frac{P_{T1}}{P_{T2}}\right)^{\frac{\gamma-1}{\gamma}}\left[1 + \frac{\gamma-1}{2} M_2^2\right] - 1\right\} \quad \text{(A-50)}$$

for $M_1 \geq 1$, set $M_1 = 1$, since the primary nozzle is convergent.

c. Density Ratio

$$\delta = \frac{\rho_2}{\rho_1} = \frac{(\rho_2/\rho_{T2})}{(\rho_1/\rho_{T1})}\frac{\rho_{T2}}{\rho_{T1}}$$

or

$$\delta = \left[\frac{1 + \frac{\gamma-1}{2} M_1^2}{1 + \frac{\gamma-1}{2} M_2^2}\right]^{1/\gamma-1}\left(\frac{P_{T2}}{P_{T1}}\right)\left(\frac{T_{T1}}{T_{T2}}\right) \quad \text{(A-51)}$$

d. Flow Rate Ratio

$$X = \frac{\dot{m}_2}{\dot{m}_1} = \frac{\rho_2 \; A_2 \; V_2}{\rho_1 \; A_1 \; V_1}$$

or

$$X = \delta^2(K^2-1) \left(\frac{M_2}{M_1}\right)\sqrt{\frac{T_2}{T_1}}$$

but

$$\frac{T_2}{T_1} = \frac{(T_2/T_{T2})}{(T_1/T_{T1})} \left(\frac{T_{T2}}{T_{T1}}\right)$$

$$= \left(\frac{T_{T2}}{T_{T1}}\right)\left[\frac{1 + \frac{\gamma-1}{2}M_1^{\,2}}{1 + \frac{\gamma-1}{2}M_2^{\,2}}\right]$$

therefore,

$$X = \delta(K^2-1) \left(\frac{M_2}{M_1}\right)\left\{\left(\frac{T_{T2}}{T_{T1}}\right) \left[\frac{1 + \frac{\gamma-1}{2}M_1^{\,2}}{1 + \frac{\gamma-1}{2}M_2^{\,2}}\right]\right\}^{1/2} \qquad \text{(A-52)}$$

e. From these inlet conditions, a value of Φ can be determined.

$$\Phi_i = \frac{P_3 - P_2}{\rho_2 \; V_1^{\,2}}$$

$$= \frac{\left(\frac{P_3}{P_1}\right) - \left(\frac{P_2}{P_1}\right)}{\frac{\rho_2}{P_1} V_1^{\,2}} = \frac{\left[\left(\frac{P_3}{P_1}\right) - \left(\frac{P_2}{P_1}\right)\right]}{\frac{\delta\rho_1}{P_1} V_1^{\,2}}$$

$$\therefore \Phi_i = \left[\left(\frac{P_3}{P_1}\right) - \left(\frac{P_2}{P_1}\right)\right] \Big/ \; \delta\gamma M_1^{\,2} \qquad \text{(A-53)}$$

look at

$$\frac{P_3}{P_1} = \left(\frac{P_3}{P_{T1}}\right)\left(\frac{P_{T1}}{P_1}\right) = \left(\frac{P_3}{P_{T1}}\right)\left[1 + \frac{\gamma-1}{2} M_1^{\,2}\right]^{\gamma/\gamma-1}$$

$$\frac{P_2}{P_1} = \frac{(P_2/P_{T2})}{(P_1/P_{T1})} \left(\frac{P_{T2}}{P_{T1}}\right) = \left(\frac{P_{T2}}{P_{T1}}\right)\left[\frac{1 + \frac{\gamma-1}{2}M_1^{\,2}}{1 + \frac{\gamma-1}{2}M_2^{\,2}}\right]^{\gamma/\gamma-1}$$

or finally,

$$\Phi_i = \left\{ \left(\frac{P_3}{P_{T1}}\right) \left(1 + \frac{\gamma-1}{2} M_1^2\right)^{\gamma/\gamma-1} - \left(\frac{P_{T2}}{P_{T1}}\right) \left[\frac{1 + \frac{\gamma-1}{2} M_1^2}{1 + \frac{\gamma-1}{2} M_2^2}\right]^{\gamma/\gamma-1} \right\} \Bigg/ \delta\gamma M_1^2 \qquad \text{(A-54)}$$

f. From the momentum definition of Φ, and by assuming an initial value of μ of unity, a value of Φ_m can be determined.

$$\Phi_m = \frac{1}{K^2} \left[\frac{1}{\delta} + \frac{\Delta P_1}{\rho_2 V_1^2} + \frac{x^2}{\delta(K^2-1)} - \frac{(1+x)(\mu\delta+x)}{\delta^2 K^2}\right] \qquad \text{(A-55)}$$

NOTE: All terms in this equation are known with the exception of $\frac{\Delta P_1}{\rho_2 V_1^2}$.

For $M_1 < 1$; $\Delta P = 0$

For $M \geq 1$;

$$\Delta P_1 = P_1 - P_2 = .528\ P_{T1} - P_2$$

and

$$P_2 = \frac{P_{T2}}{\left[1 + \frac{\gamma-1}{2} M_2^2\right]^{\gamma/\gamma-1}}$$

therefore,

$$\frac{\Delta P_1}{\rho_2 V_1^2} = \left\{.528\ P_{T1} - \frac{P_{T2}}{\left[1 + \frac{\gamma-1}{2} M_2^2\right]^{\gamma/\gamma-1}}\right\} \left[\frac{1}{\rho_2 V_1^2}\right]$$

or after some algebraic manipulation,

$$\frac{\Delta P_1}{\rho_2 V_1^2} = \frac{\left[1 + \frac{\gamma-1}{2} M_1^2\right]^{\gamma/\gamma-1}}{\delta\gamma M_1^2} \left\{.528 - \left(\frac{P_{T2}}{P_{T1}}\right) \left[\frac{1}{\left(1+\frac{\gamma-1}{2} M_2^2\right)^{\gamma/\gamma-1}}\right]\right\} \qquad \text{(A-56)}$$

thus, Φ_m is known.

g. The necessary condition for a solution is that Φ_i equal Φ_m; thus, all boundary conditions are satisfied.

let

$$ERF = \Phi_m = \Phi_i \tag{A-57}$$

Such that for a given set of parameters and a particular value of μ, the proper M_2 has been chosen when ERF = 0.

h. It is now possible to obtain a new value for μ.

From energy considerations,

$$\dot{m}_1 C_p T_{T1} + \dot{m}_2 C_p T_{T2} = \dot{m}_3 C_p T_{T3}$$

for C_p = const

$$\frac{T_{T3}}{T_{T2}} = \left[\frac{T_{T1}/T_{T2} + x}{1 + x}\right] \tag{A-58}$$

also,

$$T_{T3} = T_3 + \frac{V_3^2}{2C_p}$$

or

$$\frac{T_{T3}}{T_{T2}} = \frac{T_3}{T_{T2}} + \frac{V_3^2}{2\frac{\gamma R}{\gamma-1} T_{T2}}$$

after some rearranging,

$$\frac{T_3}{T_{T2}} = \left(\frac{T_{T3}}{T_{T2}}\right) - \left(\frac{\gamma-1}{2}\right)\left(\frac{T_{T1}}{T_{T2}}\right)\left[\frac{M_1^2}{1+\frac{\gamma-1}{2}M_1^2}\right]\left[\frac{\mu\delta+x}{\rho K^2}\right]^2 \tag{A-59}$$

from equation of state,

$$\frac{\rho_3}{\rho_2} = \frac{P_3 T_2}{P_2 T_3} = \left[\frac{P_2 + (P_2 - P_3)}{P_2}\right]\left(\frac{T_2}{T_{T2}}\right)\left(\frac{T_{T2}}{T_3}\right)$$

or finally,

$$\frac{\rho_3}{\rho_2} = \left[\frac{\frac{P_2}{\rho_2 V_1^2} + \frac{\Phi}{2}}{P_2/\rho_2 V_1^2}\right]\left(\frac{T_{T2}}{T_3}\right)\left(\frac{1}{1 + \frac{\gamma-1}{2}M_2^2}\right) \tag{A-60}$$

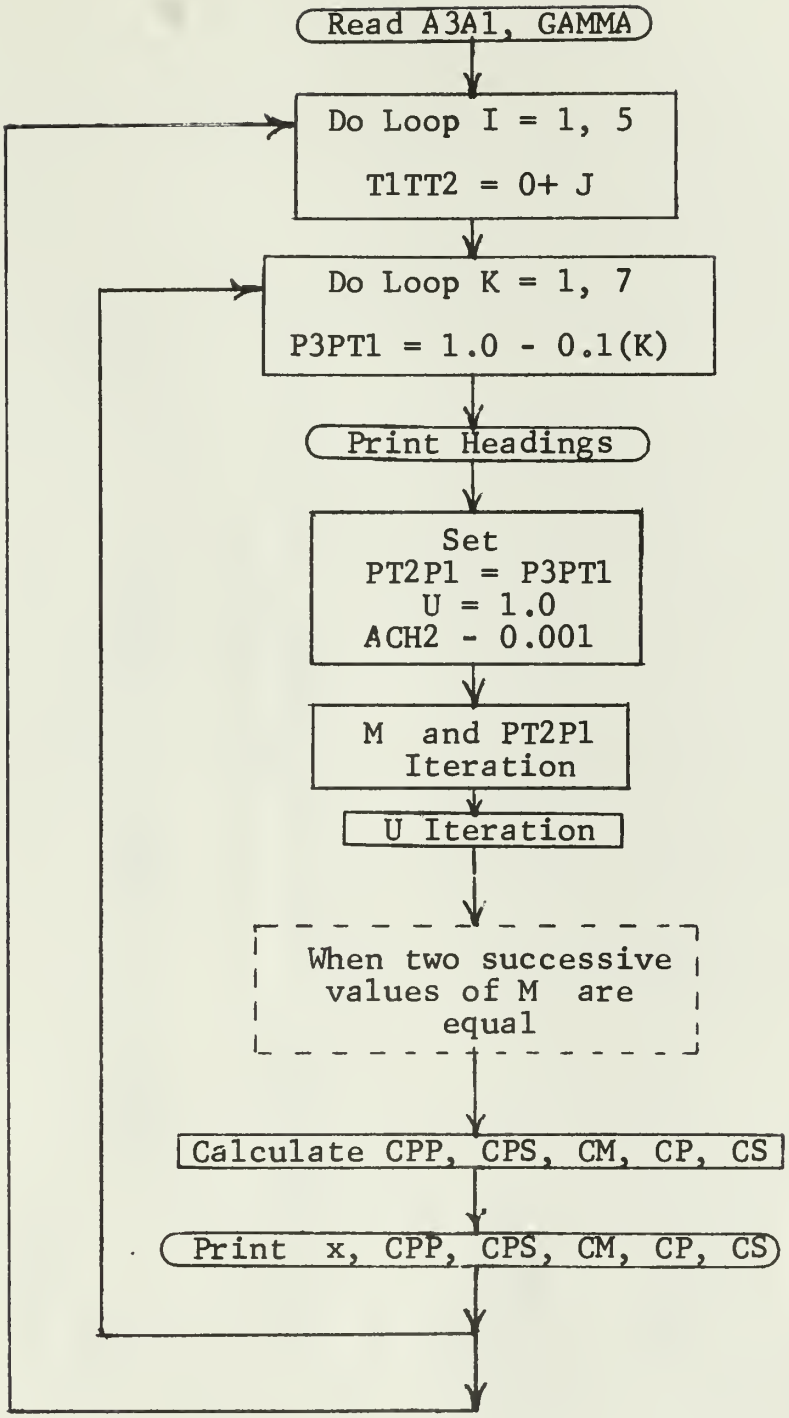
Read A3A1, GAMMA
Do Loop I = 1, 5
T1TT2 = 0+ J
Do Loop K = 1, 7
P3PT1 = 1.0 - 0.1(K)
Print Headings
Set
PT2P1 = P3PT1
U = 1.0
ACH2 - 0.001
M and PT2P1
Iteration
U Iteration
When two successive
values of M are
equal
Calculate CPP, CPS, CM, CP, CS
Print x, CPP, CPS, CM, CP, CS

```
-COOP,0234,WADE B S,S/1S/2S,30,10000.
-FTN,L,E,A.
      PROGRAM JETPUMPI
      DIMENSION Y(20)
      READ 20,A3A1,GAMMA
   20 FORMAT(2F10.5)
      GA=GAMMA/(GAMMA-1.0)
      GB=1.0/GA
      GC=1.0/(GAMMA-1.0)
      GD=(GAMMA-1.0)/2.0
      GE=(GAMMA+1.0)/2.0
      GF=1.0/GAMMA
      DO 101 J=1,5
      T1TT2=0.0
      XJ=J
      T1TT2=T1TT2+XJ
      TT2T1=1.0/T1TT2
      DO 100 K=1,7
      P3PT1=1.0
      XK=K
      P3PT1=P3PT1-0.1*XK
      PRINT 75
   75 FORMAT(1H1,39X,42HPARAMETRIC ANALYSIS OF EJECTOR PERFORMANCE,///)
      PRINT 76,A3A1,T1TT2,P3PT1
   76 FORMAT(7X,8HA3A1   = ,1F13.5,/,7X,8HTT1TT2= ,1F13.5,/,
     17X,8HP3PT1 = ,1F13.5,//)
      PRINT 77
   77 FORMAT(115H        PT2PT1         MACH1         MACH2           X
     1      GPP           CPS           CP            CM            CS)
      PT2P1=P3PT1
      YI= .1
    1 P1PT2=1.0/PT2P1
      U=1.0
      SACH2=0.0001
   15 ACH2=0.0001
      XI= .01
```

```
 9 ACH1=((1.0/GD)*(P1PT2**GB*(1.0+GD*ACH2*ACH2)-1.0))**0.5
   IF(ACH1-0.99999)17,17,16
16 ACH1=1.0
17 A=1.0+GD*ACH1*ACH1
   B=1.0+GD*ACH2*ACH2
   DEL=PT2P1*T1TT2*((A/B)**GC)
   X=DEL*(A3A1-1.0)*((A/(B*T1TT2))**0.5)*ACH2/ACH1
  0PHII=(1.0/(DEL*GAMMA*ACH1*ACH1))*(P3PT1*(A**GA)
  1-PT2P1*((A/B)**GA))
   IF(ACH1-0.99999)2,2,3
 2 DELP1=0.0
   GO TO 4
 3 DELP1=GE**GA*(.52828-PT2P1/(B**GA))/(DEL*GAMMA)
 40PHIM= 1.0/A3A1*(DELP1+ X*X/(DEL*DEL*(A3A1-1.0))+1.0/DEL
  1-(1.0+X)*(U*DEL+X)/(DEL*DEL*A3A1))
   ERF=PHIM-PHII
   IF(ACH2-.00011)30,31,31
30 IF(ERF)32,31,31
32 IF(YI-.0011)100,100,90
90 PT2P1=PT2P1+YI
   YI= .1*YI
   PT2P1=PT2P1-YI
   GO TO 1
31 IF(ABSF(ERF)-.0001)5,5,6
 5 IF(ABSF(ACH2-SACH2)-.0001)8,8,7
 6 IF(ERF)40,41,41
40 ACH2=ACH2-XI
   XI=.01*XI
   ACH2=ACH2+XI
   GO TO 42
41 ACH2=ACH2+XI
42 IF(ACH2-1.0001)9,9,100
 7 TT32=(T1TT2+X)/(1.0+X)
   DELP2=PT2P1*(1.0/(GAMMA*DEL*ACH1*ACH1))*(A/B)**GA
120T3TT2=TT32-GD*ACH1*ACH1/A*T1TT2*((U*DEL+X)/(DEL*A3A1))*((U*DEL+X)
  1/(DEL*A3A1))
```

```
      R3R2=(DELP2+PHIM)/DELP2*(1.0/TT32)*1.0/B
      UU= 1.0/DEL*((1.0+X)/R3R2-X)
      IF(ABSF(UU-U)-0.0001)10,10,11
   10 U=UU
      SACH2=ACH2
      GO TO 15
   11 U=UU
      GO TO.12
    8 PP=(1.0-T3TT2/TT32)/(1.0-P3PT1**GB)
      CPP=(1.0+X)*TT32*(1.0/T1TT2)*PP
      PS=LOGF(P3PT1*P1PT2)/(1.0-P3PT1**GB)
      CPS=X*GB*TT2T1*PS
      CPT=CPP+CPS
      CM=CPP**.5*(1.0+X)**.5
      CP=GB*TT2T1*P1PT2*(1.0-P3PT1)/(1.0 P3PT1**GB)
      CS=GB*TT2T1*(1.0-P3PT1*P1PT2)/(1.0 P3PT1**GB)
      PRINT 14,PT2P1,ACH1,ACH2,X,CPP,CPS,CP,CM,CS
   14 FORMAT(9F13.5)
   80 PT2P1=PT2P1-YI
      IF(PT2P1)100,100,1
  100 CONTINUE
  101 CONTINUE
          END
          END
          FINIS
-EXECUTE.
20.25       1.4
```

78

APPENDIX B

Experimental Development

Since the primary objective of the experimental program was to obtain a realistic comparison of actual ejector performance with the idealized theoretical predictions, the data obtained was reduced to the same non-dimensional performance coefficients as developed in the theoretical analysis. With the aid of a specific computer program, EJECTOR, the raw data was converted to obtain these required coefficients.

1. Flow rate calculations

As mentioned in Section 3, the primary and secondary flow rates were determined using squared edged orifice plates with flange pressure taps and an iron-constantan thermocouple in accordance with ASME standards.

From Reference 4,

$$\dot{m} = \frac{359.1}{3600} D_2^2 \alpha K Y \sqrt{\rho h\omega} \qquad \text{(B-1)}$$

where

$\dot{m}$ = mass flow rate

D_2 = orifice diameter

α = thermal expansion factor

Y_1 = compressibility factor

K = discharge coefficient

ρ = fluid density

$h\omega$ = pressure drop across the orifice

Now, for an ideal gas,

$$\rho = \frac{P}{RT}$$

with

P in inches of mercury

T in $^{o}_{R}$

$h\omega$ in CM H_2O

$$\dot{m} = \frac{359.1}{3600}\sqrt{\frac{(144)(.491)}{(53.345)(2.54)}}\, D_2^{\,2}\, \alpha K Y_1 \sqrt{\frac{P_1 h\omega}{T_1}}$$

$$\dot{m} = (.07205)\, D_2^{\,2}\, \alpha K Y_1 \sqrt{\frac{P_1 h\omega}{T_1}} \qquad \text{(B-2)}$$

where

T_1 = static temperature upstream of the orifice

From Reference 5, for stainless steel orifice plates operating in a temperature range of 60^{o} - 350^{o} F.

$$\alpha = 1.0 + 0.0015 \left(\frac{t_1 - 60}{100}\right) \qquad \text{(B-3)}$$

where

$$t_1 = T_1 - 460$$

therefore,

$$\alpha = 1.0 + 1.5\,(T_1 - 520) \times 10^{-5} \qquad \text{(B-4)}$$

Also, from Reference 5, the expansion factor for air with $\gamma = 1.4$,

$$Y_1 = 1.0 - \left[.041 + .035\left(\frac{D_2}{D_1}\right)^4\right] \frac{h\omega}{P\gamma} \qquad \text{(B-5)}$$

for $h\omega$ in CM of H_2O, P in Hg, $\frac{D_2}{D_1} = 0.7$

$$Y_1 = 1.0 + 0.0102\, \frac{h\omega}{P} \qquad \text{(B-6)}$$

The discharge coefficient K, was determined in order to correct for Reynolds Number effects.

$$R_E = \frac{6.316W}{D_2 \mathcal{Z}^1} \tag{B-7}$$

where

$W = 3600\ \dot{m}$

$\mathcal{Z}^1$ = absolute fluid viscosity

By determining a linear relationship between $\mathcal{Z}^1$ and t from Reference 5, page 335, it was determined that

$$\mathcal{Z} = 100\ \mathcal{Z}^1 = 1.9 + 0.24\left(\frac{t_1}{100} - 1\right) \tag{B-8}$$

or

$$\mathcal{Z} = \left[1.9 + 0.24\left(\frac{T_1}{100} - 5.6\right)\right] \times 10^{-2}$$

therefore:

$$R_E = \left\{\frac{(6.316)(3600) \times 10^2}{D_2\left[1.9+0.24\left(\frac{T_1}{100} - 5.6\right)\right]}\right\}\dot{m} \tag{B-9}$$

Now, for flange pressure taps the discharge coefficient K, can be determined

$$K = \left[1 + \frac{A}{R_E}\right] K_\infty = \zeta K_\infty \tag{B-10}$$

where

$$A = D_2\left[830 - 5000\left(\frac{D_2}{D_1}\right) + 9000\left(\frac{D_2}{D_1}\right)^2 - 4200\left(\frac{D_2}{D_1}\right)^3 + \frac{530}{\sqrt{D_1}}\right] \tag{B-11}$$

K_∞ = tabulated discharge coefficient for $R_E = \infty$.

Combining these results gives:

$$\dot{m} = C_1 K_\infty D_2^2 \alpha Y_1 \zeta \sqrt{\frac{P h_\omega}{T}} \qquad \text{(B-12)}$$

Now, for the primary air system

$C_1 = .07205$

$K_\infty = .9756$

$D_1 = 2.067$ in

$D_2 = 1.4465$ in

$$C_1^1 = C_1 K_\infty D_2^2 = 0.14707$$

$$\alpha = 1.0 + 1.5 \left(\frac{T_1}{100} - 5.2 \right) \times 10^{-5}$$

$$Y_1 = 1.0 - 0.0102 \frac{h_\omega}{D_1}$$

$$\zeta = 1 + \frac{966.324}{R_E}$$

Since ζ is dependent upon the actual flow rate, the final solution is based upon an iteration solution, where originally ζ is assumed to be unity. This iteration is performed with the CDC 1604 digital computer as is shown in the Fortran Program EJECTOR (Appendix B). The same procedure is followed in determining the secondary flow rate.

2. Average Exit Total Pressure

In order to obtain the state condition at the exit to the mixing section, a pitot-static Prandtl type pressure probe was used to traverse the exit plane. The static pressure was found to be essentially constant as was the total temperature. The total pressure, however, varied along the

traverse. For this reason, it was necessary to determine a suitable equivalent average total pressure.

Consider a hypothetical constant area, frictionless duct appended to the actual mixing section. Assume that the velocity profile changes from the given non-uniform distribution to a uniform value. Since the Mach numbers at the exit plane were less than 0.3, compressibility effects may be neglected.

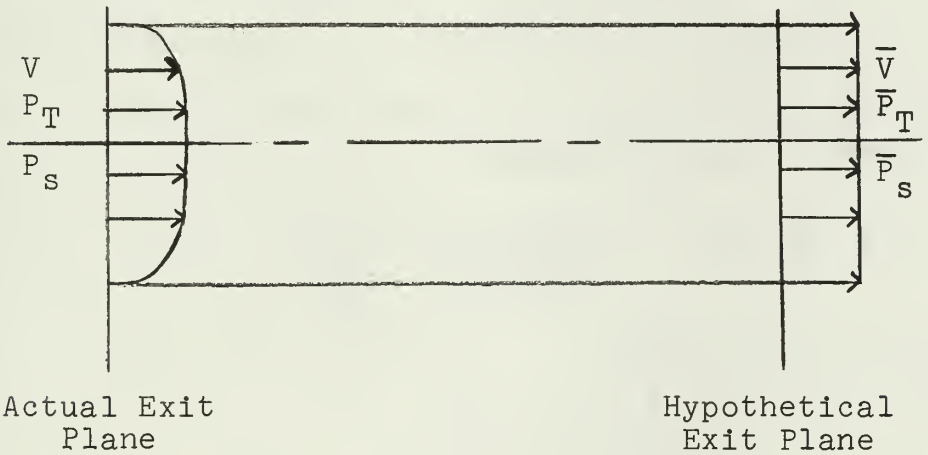

For incompressible flow:

$$P_T = P_S + 1/2\ \rho V^2$$

and

$$\overline{P}_T = \overline{P}_S + 1/2\ \rho\ \overline{V}^2 \qquad \text{(B-14)}$$

From continuity:

$$\int_A \rho\ V\ d\ A = \int_A \rho\ \overline{V}\ d\ A$$

for ρ and $\overline{V}$ = const

$$\overline{V} = \int_A V\ \frac{dA}{A} \qquad \text{(B-15)}$$

Now, applying the Momentum Equation,

$$\int P_S\ d\ A - \int \overline{P}_S\ d\ A = \int \rho\ \overline{V}^2\ d\ A - \int \rho\ V^2\ d\ A \qquad \text{(B-16)}$$

for P_s = const = 0 psig

$\bar{V}$ = const

ρ = const

$\bar{P}_s$ = const

Therefore,

$$\bar{P}_T - P_s = \bar{q} = \int \rho V^2 \frac{dA}{A} - 1/2 \rho \bar{V}^2 \qquad \text{(B-17)}$$

but

$$P_T - P_s = q = 1/2 \rho V^2$$

$$V^2 = \frac{2q}{\rho} \qquad \text{(B-18)}$$

Now, substituting for V and $\bar{V}$,

$$\bar{q} = \int \rho \frac{2q}{\rho} \frac{dA}{A} - 1/2 \rho \left[\int \left(\frac{2q}{\rho} \right)^{1/2} \frac{dA}{A} \right]^2 \qquad \text{(B-19)}$$

or, since ρ is constant

$$\bar{q} = 2 \int q \frac{dA}{A} - \left[\int q^{1/2} \frac{dA}{A} \right]^2 \qquad \text{(B-20)}$$

however, since $\bar{P}_{AMB} = P_s$

$$\bar{H}_T = 2 \int h_T \frac{dA}{A} - \left[\int h_T^{1/2} \frac{dA}{A} \right]^2 \qquad \text{(B-21)}$$

where h_T = total pressure head measure at the exit plane.

This result was then converted to a finite difference format where:

h_i = total head measured at the ith traverse

ΔA_i = annulus areas corresponding to the ith traverse station

therefore,

$$\bar{H}_T = 2\Sigma h_i \frac{\Delta A_i}{A} - \left[\Sigma h_i^{1/2} \frac{\Delta A_i}{A} \right]^2 \qquad \text{(B-22)}$$

After checking several calculations it was found that:

$$\left[\Sigma\ h_i^{1/2}\ \frac{\Delta A_i}{A}\right]^2 \cong \Sigma\ h_i\ \frac{\Delta A_i}{A} \qquad \text{(B-23)}$$

The approximation was then made that

$$\overline{H}_T = \quad h_i\ \frac{\Delta A_i}{A} \qquad \text{(B-24)}$$

This approximation gives an error of less than two percent for the worst case.

3. Performance Coefficients

Upon determining the individual flow rates and measuring the conditions at the exit plane, it was possible to calculate all performance coefficients.

a. Pumping Power Coefficient

$$C_{pp} \triangleq \frac{(\dot{m}_1 + \dot{m}_2)\ H_3}{\dot{m}_1\ H_a}$$

$$C_{pp} = (1 + x)\left(\frac{T_{T3}}{T_{T1}}\right)\left\{\frac{1-\left(\frac{P_3}{P_{T3}}\right)^{\frac{\gamma-1}{\gamma}}}{1-\left(\frac{P_3}{P_{T1}}\right)^{\frac{\gamma-1}{\gamma}}}\right\} \qquad \text{(B-25)}$$

NOTE: Both T_{T3} and T_{T_1} were measured directly along with P_{T1}. P_{T3} was determined from previous analysis (Section 2) while P_3 was ambient pressure.

b. Suction Power Coefficient

$$C_{ps} \triangleq \frac{\dot{m}_2\ H_s}{\dot{m}_1\ H_a}$$

$$C_{ps} = \frac{x\left(\frac{\gamma-1}{\gamma}\right)\left(\frac{T_{T2}}{T_{T1}}\right)\ \ell n\left(\frac{P_3}{P_{T2}}\right)}{\left[1\ -\left(\frac{P_3}{P_{T1}}\right)^{\frac{\gamma-1}{\gamma}}\right]} \qquad \text{(B-26)}$$

c. Output Momentum Coefficient

$$C_M \triangleq \frac{(\dot{m}_1 + \dot{m}_2)\, V_3}{\dot{m}_1 \sqrt{H_a}}$$

$$= (1 + x) \sqrt{\frac{2H_3}{H_a}}$$

$$C_M = (2\, C_{pp})^{1/2}\, (1 + x)^{1/2} \qquad \text{(B-27}$$

d. Driving Pressure Coefficient

$$C_p \triangleq \frac{P_{T1} - P_3}{\rho_{T2}\, H_a}$$

$$= \frac{P_{T1} - P_3}{\left(\frac{P_{T2}}{RT_{T2}}\right) C_p\, T_{T1} \left[1 - \left(\frac{P_3}{P_{T1}}\right)^{\frac{\gamma-1}{\gamma}}\right]}$$

or, finally,

$$C_p = \left(\frac{\gamma-1}{\gamma}\right)\left(\frac{T_{T2}}{T_{T1}}\right)\left(\frac{P_{T1}}{P_{T2}}\right)\left[\frac{1 - \frac{P_3}{P_{T1}}}{1 - \left(\frac{P_3}{P_{T1}}\right)^{\frac{\gamma-1}{\gamma}}}\right] \qquad \text{(B-28)}$$

e. Suction Pressure Coefficient

$$C_s = \frac{P_{T2} - P_3}{\rho_{T2}\, H_a}$$

$$= \frac{(P_{T2} - P_3)}{\left(\frac{P_{T2}}{RT_{T2}}\right) C_p\, T_{T1} \left[1 - \left(\frac{P_3}{P_{T1}}\right)^{\frac{\gamma-1}{\gamma}}\right]}$$

or,

$$C_s = \left(\frac{\gamma-1}{\gamma}\right)\left(\frac{T_{T2}}{T_{T1}}\right)\left[\frac{P_{T2} - P_3}{1 - \left(P_3/P_{T1}\right)^{\frac{\gamma-1}{\gamma}}}\right] \qquad \text{(B-29)}$$

These coefficients were calculated from the experimental data with a rather basic data reduction program EJECTOR as will be shown in the following section.

4. Data Reduction Program -- EJECTOR

The following is a comparison listing of Fortran symbols to the actual Algebraic symbols used throughout this study:

Algebraic	Fortran	Remarks
K^2	A3A1	Ratio of the mixing section area to the primary nozzle area.
TARE	TARE	Manometer atmospheric reference.
Pamb	PAMB	Atmospheric pressure in inches of mercury.
γ	GAMMA	Ratio of specific heats.
	H(I)	Recorded pressure readings at Station I.
T_1	T1	Primary temperature recorded upstream of the orifice plate.
T_2	T2	Secondary temperature recorded upstream of the orifice plate.
T_{Ti}	TT(I)	Total temperature at Station I.
P_i	P(I)	Absolute pressure at Station I.
$\dot{m}_1$	XP1	Primary mass flow rate.
$\dot{m}_2$	XS1	Secondary mass flow rate.
M_2	ACH2	Secondary fluid mach number at the entrance to the mixing section.
P_{T2}/P_{T1}	PT2P1	Ratio of the secondary-to-primary total pressures.
T_{T2}/T_{T1}	TT2T1	Average exit total temperatures.
P_{T3}	P(12)	Average exit total pressure.

Algebraic	Fortran	Remarks
x	X	Ratio of secondary-to-primary mass flow rates.
C_{pp}	CPP	Pumping power coefficient.
C_{ps}	CPS	Suction power coefficient.
C_{p}	CP	Driving pressure coefficient.
C_{s}	CS	Suction pressure coefficient.
C_{m}	CM	Momentum coefficient.

The program, EJECTOR, was set up to read in any number of sets of data. For each set, a new value of A3A1, PAMB, TARE, and GAMMA must be read. The program consists of two overall do loops combining the two flow rate iterations and the calculation of all required coefficients. The logic flow chart and Fortran program are shown on the following pages.

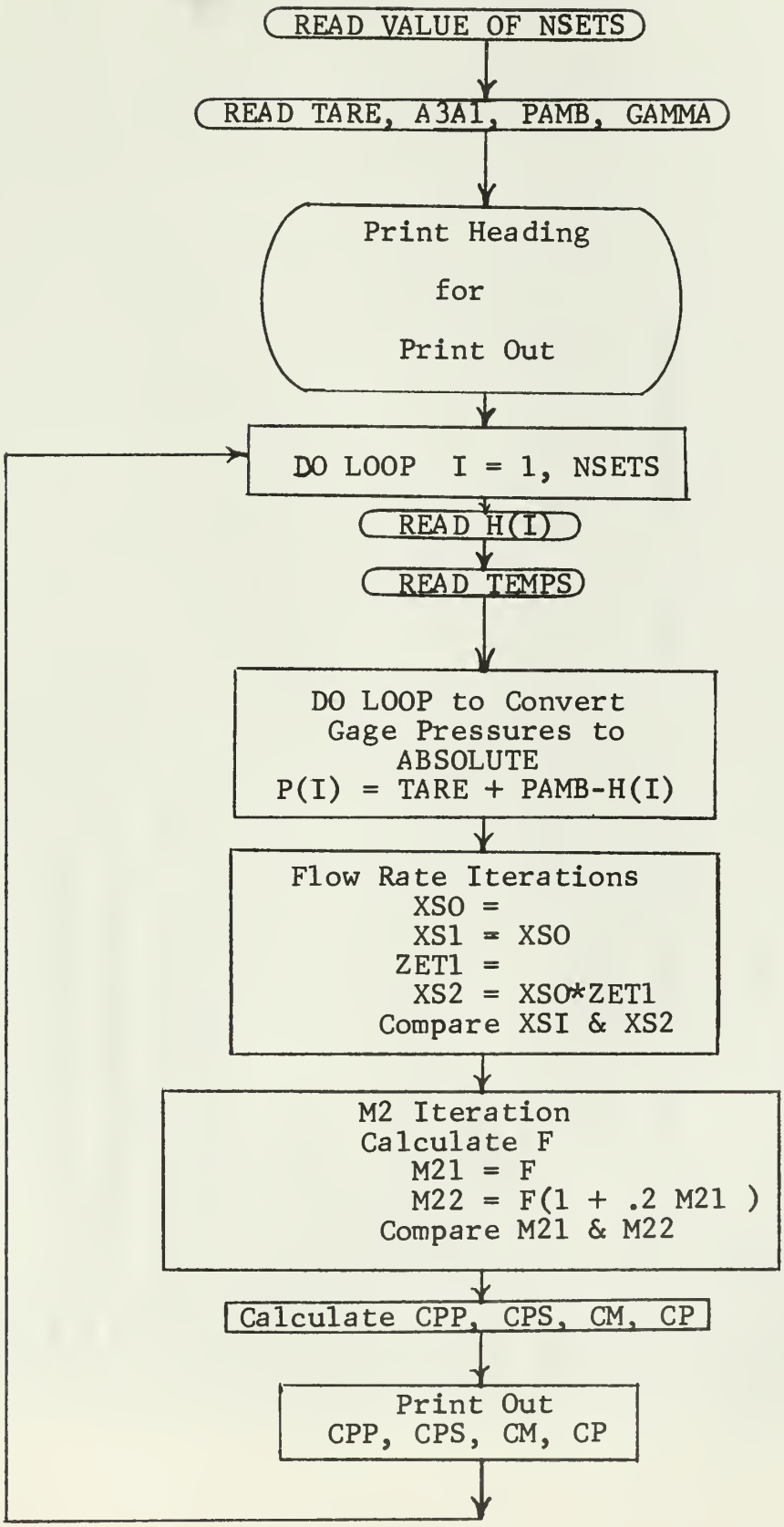
READ VALUE OF NSETS
READ TARE, A3A1, PAMB, GAMMA
Print Heading
for
Print Out
DO LOOP I = 1, NSETS
READ H(I)
READ TEMPS
DO LOOP to Convert
Gage Pressures to
ABSOLUTE
P(I) = TARE + PAMB-H(I)
Flow Rate Iterations
XSO =
XS1 = XSO
ZET1 =
XS2 = XSO*ZET1
Compare XSI & XS2
M2 Iteration
Calculate F
M21 = F
M22 = F(1 + .2 M21)
Compare M21 & M22
Calculate CPP, CPS, CM, CP
Print Out
CPP, CPS, CM, CP

```
-COOP,0234,WADE B S,S/1S/2S,10,10000.
-FTN,L,E.
      PROGRAM EJECTOR1
      DIMENSION H(12),P(12)
      READ 1,NSETS
    1 FORMAT(I3)
      READ 2,A3A1,TARE,PAMB,GAMMA
    2 FORMAT(4F10.5)
      PRINT 3
    3 FORMAT(1H1,38X,44HEXPERIMENTAL ANALYSIS OF EJECTOR PERFORMANCE,//)
      PRINT 4,A3A1
    4 FORMAT(11H     A3A1= ,1F12.4,///)
      PRINT 5
   50FORMAT(118H        P3PT1       PT2PT1        M1            M2
     1 X            CPP          CPS          CP            CM            MU ,)
      DO 200 I=1,NSETS
      READ 6,(H(J),J=1,12)
    6 FORMAT(12F6.3)
      READ 7,T1,T2,TT1,TT2,TT3
    7 FORMAT(5F10.5)
      DO 8 K=1,12
      P(K)=TARE+PAMB-H(K)
    8 CONTINUE
      C1=.14707
      ALPH1=1.0+.0015*(.01*T1-5.2)
      Y11=1.0-0.0102*H(9)/P(8)
      XP0=C1*ALPH1*Y11*(P(8)*H(9)/T1)**.5
      XP1=XP0
    9 ZET1=1.0+.00061*(1.9+.24*(.01*T1-5.6))/XP1
      XP2=XP0*ZET1
      IF(ABSF(XP1-XP2)-.0001)10,10,11
   11 XP1=XP2
      GO TO 9
   10 XP1=XP2
      C2=.32419
      ALPH2=1.0+.0015*(.01*T2-5.2)
```

```
      Y12=1.0-.0102*H(11)/P(10)
      XS0=C2*ALPH2*Y12*(P(10)*H(11)/T2)**.5
      XS1=XS0
   12 ZET2=1.0+.00175*(1.9+.24*(.01*T2-5.6))/XS1
      XS2=XS0*ZET2
      IF(ABSF(XS1-XS2)-.0001)13,13,14
   14 XS1=XS2
      GO TO 12
   13 XS1=XS2
      X=XS1/XP1
      PT2P1=P(2)/P(1)
      P1PT2=1.0/PT2P1
      P3PT1=PAMB/P(1)
      T1TT2=TT1/TT2
      TT2T1=1.0/T1TT2
      PT3=P(12)
      TT31=TT3/TT1
      GA=(GAMMA-1.0)/GAMMA
      GB=1.0/GA
      GC=1.0/(GAMMA-1.0)
      A2=3.583494
      F=XS1/(A2*P(2))*2.213*TT2**.5
      ACH21=F
   59 ACH22=F*(1.0+ACH21*ACH21)**3.0
      IF((ACH22-ACH21)-.001)60,60,70
   70 ACH21=ACH22
      GO TO 59
   60 ACH21=ACH22
      B=1.0+.2*ACH21*ACH21
      PP=GA*(P(1)-PAMB)*B**GC
      CPP=(1.0+X)*TT31*(1.0-(PAMB/PT3)**GA)/(1.0-P3PT1**GA)
      CPS=X*GA*LOGF(PAMB/P(2))/(1.0-P3PT1**GA)
      CM=CPP**.5*(1.0+X)**.5
      CP=GB*TT2T1*P1PT2*(1.0-P3PT1)/(1.0 P3PT1**GB)
      CS=GB*TT2T1*(1.0-P3PT1*P1PT2)/(1.0 P3PT1**GB)
      PRINT 15,P3PT1,PT2P1,XP1,XS1,X,CPP,CPS,CP,CM,U
```

```
   15 FORMAT(10F12.4)
  200 CONTINUE
         END
         END
         FINIS
-EXECUTE.
```

INITIAL DISTRIBUTION LIST

		No. Copies
1.	Defense Documentation Center Cameron Station Alexandria, Virginia 22314	20
2.	Library Naval Postgraduate School Monterey, California 93940	2
3.	Commander Naval Air Systems Command Department of the Navy Washington, D. C. 20360	1
4.	Professor T. H. Gawain Department of Aeronautics Naval Postgraduate School Monterey, California 93940	2
5.	LT B. S. Wade, USNR Attack Squadron FIVE TWO Fleet Post Office San Francisco, California 96601	1
6.	Chairman, Department of Aeronautics Naval Postgraduate School Monterey, California 93940	1

DOCUMENT CONTROL DATA - R&D

(Security classification of title, body of abstract and indexing annotation must be entered when the overall report is classified)

1. ORIGINATING ACTIVITY (Corporate author)

Naval Postgraduate School
Monterey, California 93940

2a. REPORT SECURITY CLASSIFICATION

UNCLASSIFIED

2b. GROUP

3. REPORT TITLE

PARAMETRIC AND EXPERIMENTAL ANALYSIS OF EJECTOR PERFORMANCE

4. DESCRIPTIVE NOTES (Type of report and inclusive dates)

Master of Science Thesis in Aeronautical Engineering

5. AUTHOR(S) (Last name, first name, initial)

Wade, Barton S.
Lieutenant, United States Naval Reserve

6. REPORT DATE	7a. TOTAL NO. OF PAGES	7b. NO. OF REFS
July 1967	94	7

8a. CONTRACT OR GRANT NO.	9a. ORIGINATOR'S REPORT NUMBER(S)
b. PROJECT NO.	
c.	9b. OTHER REPORT NO(S) (Any other numbers that may be assigned this report)
d.	

10. AVAILABILITY/LIMITATION NOTICES

11. SUPPLEMENTARY NOTES	12. SPONSORING MILITARY ACTIVITY
	Commander Naval Air Systems Command

13. ABSTRACT

This investigation analyzes the operating characteristics of an ejector having a heated primary jet and a constant area mixing section. The effects of several key parameters are determined on the basis of idealized theory. Performance characteristics are described in terms of certain non-dimensional coefficients obtained by a systematic dimensional analysis.

In addition, experimental results obtained from a model ejector are presented. These results are in reasonable agreement with the theoretical analysis.

Suggestions are made for further improvements both in the theory and in the experimental facility.

DD FORM 1 JAN 64 1473

14 KEY WORDS	LINK A		LINK B		LINK C	
	ROLE	WT	ROLE	WT	ROLE	WT
(1) Jet Pump						
(2) Ejector						
(3) Constant Area Mixing						
(4) Heated						
(5) Compressible Mixing						
(6) Performance						

thesW14
DUDLEY KNOX LIBRARY
3 2768 00415825 3
DUDLEY KNOX LIBRARY